CHIMIA

CHIMIA 2020, Volume 74
ISSN 0009-4293
www. chimia.ch
Supplementa to Issue 7-8/2020

SCS
Swiss Chemical
Society

SCS Fall Meeting 2020 (online conference)
Lecture, Short Talk and Poster Abstracts

Session of Inorganic & Coordination Chemistry

August 25, 2020
University of Bern (online conference)
http://scg.ch/fallmeeting/2020

Swiss Chemical Society
Haus der Akademien
Postfach
3001 Bern
Switzerland
info@scg.ch
www.scg.ch

Casale Strategy in ammonia synthesis: How to use engineering solutions to exploit the maximum benefits of the catalysts

P. Biasi[1,2], E. Filippi[1]

[1]Casale SA, Lugano, Switzerland, [2] p.biasi@casale.ch

CASALE is a global supplier of technologies and engineering solutions for the production of Ammonia, Urea, Methanol, Nitrates, Phosphates, complex fertilizers, Syngas and Melamine. With a large number of revamping projects successfully carried out in the last decades, CASALE is now the world leader in plant revamping and its technologies are installed in many ammonia, urea and methanol plants all over the world. Among all the activities, ammonia technology is the first and the most important core business of Casale.

Catalytic ammonia synthesis from H_2 and N_2 represents one of the most important industrial reactions today and despite the Haber-Bosch process being more than 100 years old [1], only slight improvements have been achieved until recently. The reaction $3H_2 + N_2 = 2NH_3$ ($\Delta H°_{298}$ = -92 kJ/mol) is favoured by higher pressure according to the Chatelier principle and, as it is an exothermic reaction, the lower the temperature the better the equilibrium concentration of ammonia. CASALE along the years has worked to optimize the performances of the catalyst-reactor symbiosis. The technology developed to maximize the performances of the ammonia synthesis catalyst developed by CASALE was the axial-radial reactor (Figure 1).

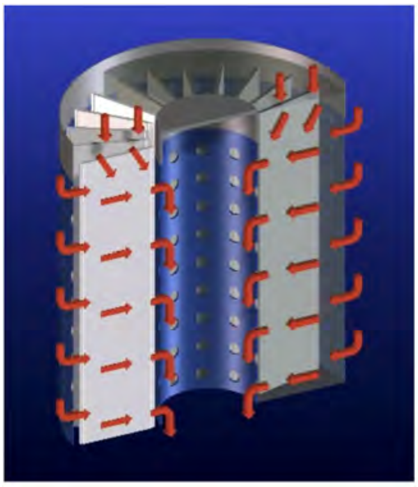

Figure 1: Axial-radial reactor

For this reason, the design of ammonia converter is a demanding chemical engineering task and Casale has always invested in the research for a new type of reactor that could valorise the performance of the catalyst. Recently Casale has developed together with CLARIANT the new Amomax-CASALE catalyst, that together with a new proprietary CASALE design for ammonia converters, allows to maximize the production of ammonia.

Therefore, through the understanding of the performance of the catalyst it is possible to improve and optimize the design of the reactor, offering new engineering solutions to valorise the catalyst and the entire process.

[1] L. Huazhang, *Chem. Industry Press*, **2013**

Synthesis and structural characterization of sodalite nanosheets and their films

M. Dakhchoune[1], K. V. Agrawal[1]*

[1]Laboratory of Advanced Separations (LAS), ISIC, EPFL

The synthesis of zeolite membranes for energy-efficient gas separation under thermally and chemically harsh conditions for several decades [1]. However, their implementation in the gas and vapor separations has been hampered because of the reproducibility issue arising from the complex hydrothermal synthesis route and the defect formation during the activation step [2]. The synthesis of molecular-sieving zeolitic membranes by the assembly of high-aspect ratio and crystalline nanosheets as building-blocks can help the scalability and reproducibility since the hydrothermal step is not required [3]. However, the intersheet gaps tend to dominate the overall transport leading to poor performance unless the undesired secondary-growth step is performed.

Herein, we report the exfoliation of the layered zeolite precursor of sodalite, RUB-15, into single 0.8 nm-thick nanosheets hosting hydrogen-sieving six-membered (6-MR) rings of SiO_4 tetrahedra and their assembly by simple filtration into thin films for H_2 sieving (Fig. 1d) yielding H_2/CO_2 over 100 [4]. RUB-15 layers were synthesized *via* hydrothermal synthesis route using a modified method reported by Gies and co-workers [5]. Swelling of RUB-15 with a C_{16} cationic surfactant was performed to increase the interlayer *d*-spacing and weaken the interlayer interactions. Finally, to overcome the electrostatic binding energy, which holds the nanosheets together, melt-compounding technique was employed (Fig. 1a) [6]. As-filtered membranes showed a periodical arrangement of the nanosheets along the z-axis with a *d*-spacing of 11.4 Å (Fig. 1b and 1e blue). Intersheet gaps dominated the overall transport leading to a cut-off in the kinetic diameter of 3.6 Å yielding H_2/N_2 selectivities over 20, while CO_2 was able to pass between the gallery spacings. The presence of reactive terminal silanol groups in the RUB-15 nanosheets presented a unique opportunity for the elimination of the nanosheets gaps. Neighboring silanol groups (Si-OH) could be condensed by heating to form covalent Si-O-Si bonds, reducing the *d*-spacing to 7.4 Å and blocking the molecular transport along these gaps (Fig. 1c and 1e red). Upon calcination, the dominated transport was through the 6-MR yielding H_2/CO_2 in the range 20-100 and H_2 permeance in the range 41-1000 GPU at 25-300 ºC and were stable for 100 h under the presence of 4% volume of water vapor at 200 °C (Fig. 1f).

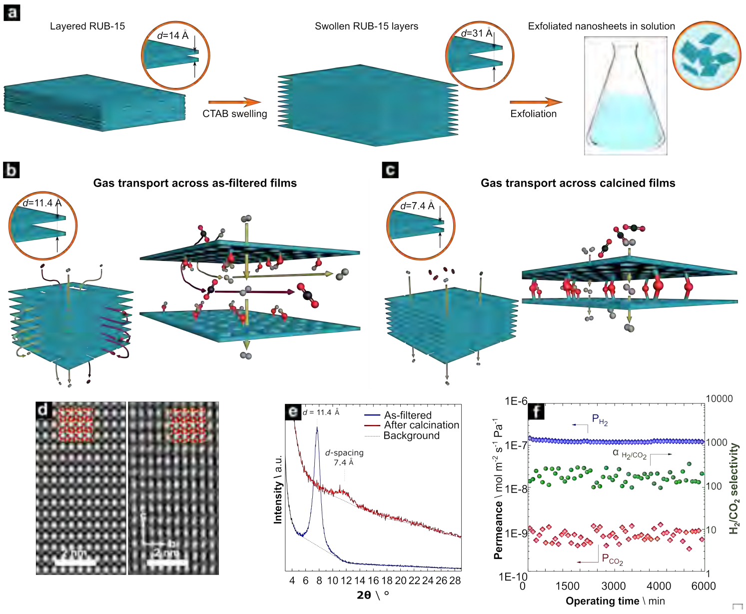

Figure 1. a) Synthesis, swelling and exfoliation of RUB-15 . **b)** Assembly of nanosheets into membrane by filtration. Nanosheets periodically arrange with *d*-spacing of 11.4 Å allowing CO_2 transport between nanosheets galleries. **c)** After calcination the *d*-spacing decreases to 7.4 Å hindering CO_2 transport. **d)** HRTEM, left: projected potential map along [100] direction of RUB-15 with a pont spread function of 2 A. Right: contrast transfer function (CTF)-corrected image. **e)** Out-of-plane XRD pattern of RUB-15 films before and after calcination. **f)** 100 h stability test with an equimolar H_2/CO_2 mixture feed in the presence of 4% of water vapor at 200 °C.

References

[1] Rangnekar N. et al., Chem. Soc. Rev. **2015**, 44, 7128-7154.
[2] Gascon J. et al., Chem. Mater. **2012**, 24, 2829-2844.
[3] Tosheva L. et al., Chem. Soc. Rev. **1996**, 17, 2494-2513
[4] Dakhchoune M. et al., under review.
[5] Oberhagemann et al., Angew.Chemie Int. Ed., 1996, 35, 2869-2872.
[6] Varoon K. V. et al., Science, **2011**, 334

Graphene nanoflake antibody conjugates for multi-modal imaging

J. Lamb[1], C. Salzmann [2], J. P. Holland[1]*

[1]University of Zurich, Department of Chemistry, [2]University College London

Graphene nanoflakes (GNFs) consist of a graphene sheet approximately 30 nm in diameter with a pristine aromatic system and an edge terminated with carboxylic acid groups.[1,2] The high water solubility, negative zeta potential, and relative ease of functionalisation using carboxylate chemistry means that GNFs are ideal scaffolds for multi-functionalisation. Our previous work demonstrated that GNFs can be loaded with the Glu-NH-C(O)-NH-Lys prostate-specific membrane antigen (PSMA) binding motif, a potent anti-mitotic drug (*R*)-ispinesib, and the chelate desferrioxamine B (DFO), to create theranostic agents.[3] Here, GNFs were functionalised with a variety of compounds including GdDOTAGA for MRI imaging, DFO for ^{89}Zr-radiolabelling for positron emission tomography imaging and BODIPY for fluorescent imaging. Constructs were tagged to the tumour targeting mAb, trastuzumab, creating a biological targeted platform for fluorescence and PET/MR imaging.

Amide coupling chemistry was successfully adapted to functionalise the GNFs with DFO, GdDOTAGA or BODIPY. Functionalised GNFs were purified on silica gel and then coupled to trastuzumab using EDC/NHS. Fluorescence assisted cell sorting (FACS) analysis using the fluorescent BODIPY-GNF-mAb construct indicated that cells selectively bind to HER2/*neu* expressing cell lines. A 2.5-fold increased uptake in the SKOV-3 cell line was seen in BODIPY-GNF-mAb compared to BODIPY-GNF, confirming that the GNF does not prevent binding to the target HER2/*neu*. The DFO-GNF-mAb construct was radiolabelled with ^{89}Zr (RCY = 27.6%, isolated RCP = 86.4%) and subsequent Lindmo cellular assay indicated binding to SKOV-3 cells with immunoreactivity of 35.7±8.0%. Preliminary PET imaging in athymic nude mice bearing a subcutaneous SKOV-3 tumour, indicated significant tumour uptake. A DFO-DOTAGA-GNF-mAb construct has also been synthesised. Radiolabelling, cellular assays and in vivo imaging will evaluate the potential of the construct as a multi-modality PET/MR imaging agent.

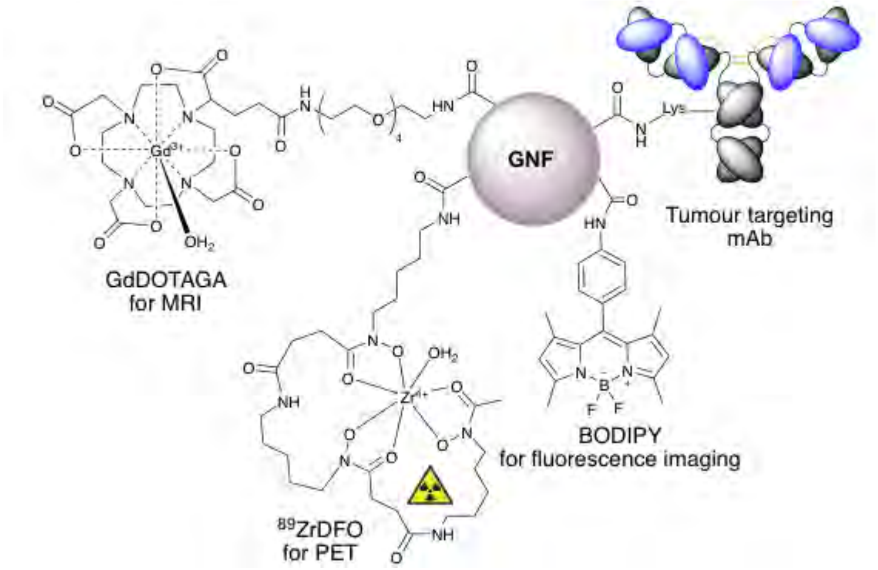

[1] C. G. Salzmann and M. L. H. Green, *J. Mater. Chem.*, 2010, **20**, 314–319.
[2] M. Rosillo-lopez, J. Lee, M. Bella, M. Hart and C. G. Salzmann, *RSC Adv.*, 2015, **5**, 104198–104202.
[3] J. Lamb, E. Fischer, M. Rosillo-Lopez, C. G. Salzmann and J. P. Holland, *Chem. Sci.*, 2019,**10**, 8880-8888

Alkali-Metal-Mediated Ferration (*AMM*Fe): Synthetic and Structural Studies with Fluoroarenes and Beyond

L. C. Maddock[1], E. Hevia[1]*

[1]Department of Chemistry and Biochemistry, Universität Bern, Freiestrasse 3, 3012, Bern,
Switzerland

Deprotonative metallation constitutes one of the most powerful methods to functionalise aromatic molecules. These reactions are usually performed by polar *s*-block metal bases such as lithium amides or alkyllithiums.[1] Previous studies have shown that building bimetallic bases combining an alkali-metal with a lower polarity main group metal, like Zn or Mg, it is possible to promote low polarity metallations.[2]

Expanding cooperative bimetallic chemistry into new territory, this contribution will report the first examples of direct ferration of sensitive fluoroaromatics.[3] By pairing sodium and iron (II) within the same molecular scaffold a powerful base has been developed, which enables direct Fe-H exchange reactions to occur selectively and in excellent yields. Key aspects controlling this unique reactivity, including the *modus operandi* of this Na/Fe bimetallic partnership, the key role of the alkali-metal as a facilitator of the ferration process as well as the influence of solvent effects will also be discussed.

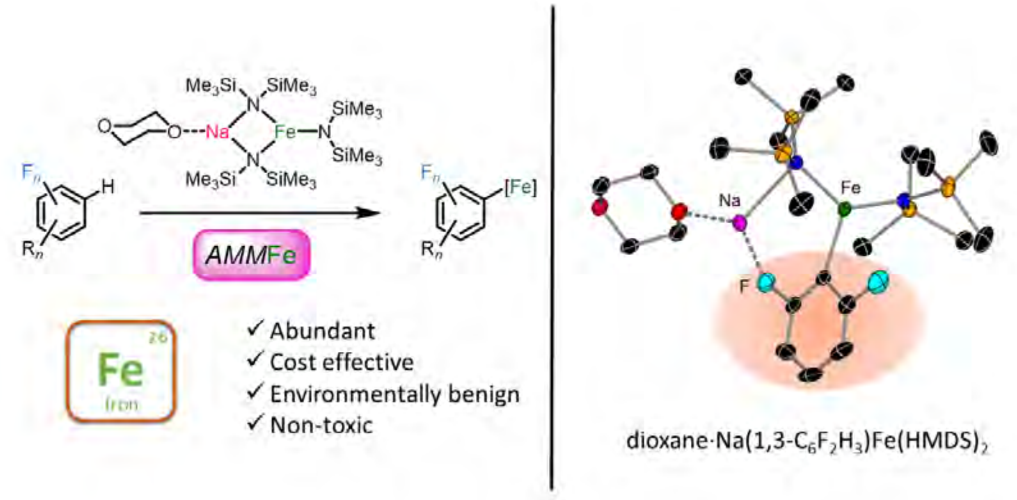

[1] M. Schlosser in *Organometallics in Synthesis: A Manual* (Ed.: M. Schlosser), Wiley, Chichester, **2002**, 1–352.
[2] R. E. Mulvey, F. Mongin, M. Uchiyama, Y. Kondo, *Angew. Chem. Int. Ed.* **2007**, *46*, 3802–24.
[3] L. C. H. Maddock, T. Nixon, A. R. Kennedy, M. R. Probert, W. Clegg, E. Hevia, *Angew. Chem. Int. Ed.* **2018**, *57*, 187–191.

From water-stable uranyl(V) to uranium(IV) polyoxometalates.

R. Faizova[1], L. Chatelain[1], R. Bernier-Latmani[1], A. Chauvin[1], F. Fadaei-Tirani[1], R. Scopelliti[1], M. Mazzanti[1]*

[1]Swiss Federal Institute of Technology Lausanne (EPFL)

Traditionally pentavalent uranyl was thought of as a highly unstable species of limited environmental importance because of the tendency of aqueous U(V) to disproportionate under most Eh-pH conditions. However, in the last decade, it has been demonstrated that uranyl(V) is a persistent intermediate in the biological and abiotic transformation of soluble uranyl(VI) compounds into insoluble uranium(IV) species (UO_2 or U(IV) discrete clusters).

In particular, U(V) is often found in association with Fe-containing minerals such as goethite and magnetite. Besides the importance of this process for ground-water remediation, the role of U(V) remains unclear as there is no appropriate synthetic model to perform the required studies.

The first example of a stable uranyl(V) complex in organic media was reported more than 10 years ago, inspiring very fast development in the field, but none of the reported compounds have shown stability in aqueous media at environmentally relevant pH.

We will present the synthesis of the first uranyl(V) complex that is stable in both organic and aqueous media. This was achieved by using an aminopicolinate ligand, combining the pentadentate binding mode with the ability to form stable complexes with metal ions in water.[1] Additionally, the effect of Fe^{2+} on the stability of U(V) toward proton induced disproportionation and redox reactions was investigated. Cation-cation interaction between uranyl(V) oxygen and Fe^{2+} was shown to play an important role in the stabilization of U(V).[2] Further, the formation of discrete uranium(IV) clusters of various nuclearities (U6 – U38) and the time dependence of the assembly of uranium oxo clusters in hydrolytic conditions in organic solvent will also be demonstrated.[3] Finally, the first example of direct conversion of a uranyl(VI) complex to a well-defined molecular U(IV) oxo/hydroxo cluster in aqueous conditions will be presented.[4]

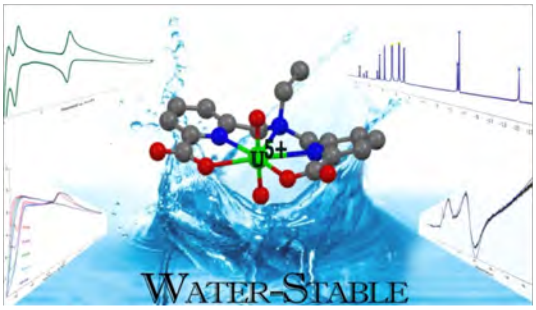

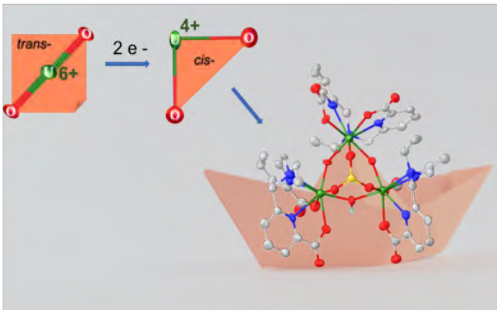

[1] Radmila Faizova, Rosario Scopelliti, Anne-Sophie Chauvin, Marinella Mazzanti, *Journal of American Chemical Society* **2018**, 140, 13554-13557.
[2] Radmila Faizova, Sarah White, Rosario Scopelliti, Marinella Mazzanti, *Chemical Science* **2018**, 9, 7520-7527.
[3] Lucile Chatelain, Radmila Faizova, Farzaneh Fadaei-Tirani, Jacques Pécaut, Marinella Mazzanti, *Angewandte Chemie International Edition* **2019**, 58, 3021-3026.
[4] Radmila Faizova, Farzaneh Fadaei-Tirani, Rizlan Bernier-Latmani, Marinella Mazzanti, *Angewandte Chemie International Edition* **2020**, 59, 6756-6759.

Polymorphism and Polytypism in the NbS_2 System

C. Witteveen[1,2], F. O. von Rohr[1,2]

[1]Department of Chemistry, University of Zurich, CH-8057 Zurich, Switzerland , [2]Department of Physics, University of Zurich, CH-8057 Zurich, Switzerland

NbS_2 is a metallic layered transition metal dichalcogenide. While the layers consist of covalently bound atoms, weak van der Waals forces hold the layers together. The layer can have two different stacking sequences, resulting in two different stable polytypes: 2H– and 3R–NbS_2. In this work, the formation of those two polytypes has been analyzed for a solid-state reaction of a fixed duration of three days. A phase diagram was established after careful PXRD analysis, and the normal-state and superconducting properties of a phase pure 2H and 3R sample, as well as of a mix of both, have been analyzed and compared. The here obtained synthesis parameters allow for an improved control of the phase purity and phase formation in the NbS_2 system.

Making, Breaking, and Elucidating Uranium-Nitrogen Multiple Bonds

S. C. Bart[1], T. S. Collins[1], E. Coughlin[1], M. Zeller[1]

[1]H.C. Brown Laboratory, Purdue University, West Lafayette, Indiana, 47906 (USA)

Redox active ligands have proven to be versatile frameworks for transition metals due to their ability to support low-valent metals in a variety of oxidation states.[1] Our laboratory has demonstrated such ligands are effective at mediating organometallic and multi-electron transfer reactions at low-valent uranium centers. Recently, we have synthesized tetravalent uranium complexes with reduced pyridine(diimine) ligands.[2] The electrons stored in these ligands facilitate multi-electron reactivity, enabling the synthesis of unprecedented uranium imido $[U(NR)_x]$ complexes with unique electronic structures. Accordingly, these results will be contrasted with attempts to generate these unique species in the absence of the redox-active ligand. Independent syntheses have been developed for new imido complexes with no ancillary ligands.[3,4] Overall, these species show loading imido substituent on a single metal center results in very activated U=N bonds. Full characterization of the multiply bonded species, including interesting structural parameters, will also be discussed.

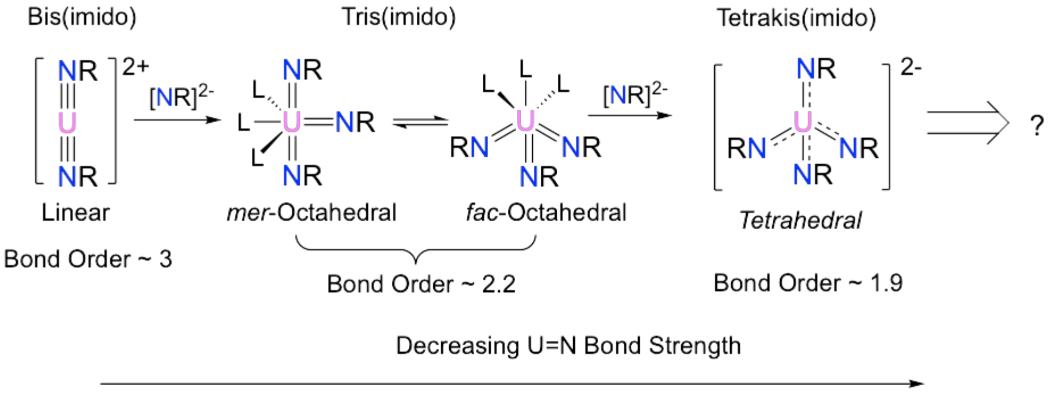

Figure 1. Trends in U=N Bonds in a Family of Uranium Imido Species.

[1] De Bruin, B.; *et al., Inorg. Chem.* **2000**, 39, 2936-2947.
[2] Anderson, N. H.; *et al., Nat. Chem.* **2014**, 6, 919-926.
[3] Anderson, N. H.; *et al., Angew. Chem., Int. Ed.* **2015**, 54, 9386-9389.
[4] Anderson, N. H.; *et al., Nat. Chem.* **2017**, 9, 850-855.

Radiochemistry at PSI and the Chemistry of Transactinide Elements

P. Steinegger[1]

[1]Laboratory of Radiochemistry, Paul Scherrer Institut, Forschungsstrasse 111, 5232 Villigen PSI

About a third of all existing elements today do not have a stable isotope and are thus radioactive (see Fig. 1). Furthermore, if we take a look at all known isotopes of all known elements, a vast majority of more than 90% are in fact radioactive (see Fig. 1). Chemistry experiments with these radionuclides are subject of nuclear and radiochemistry. The corresponding, diverse activities in Switzerland range from fundamental topics regarding the chemistry of transactinide elements or the determination of high-precision nuclear data, such as half-lives or neutron capture cross sections, to more applied fields like nuclear waste separation and disposal, research on generation IV nuclear power reactors, radiopharmaceutical sciences and nuclear forensics. Here a short overview of the radiochemical activities of the Laboratory of Radiochemistry at the Paul Scherrer Institute (PSI) is presented together with a second part focusing on chemistry experiments with transactinide elements, i.e., the newest members of the periodic table of elements. The chemical characterization of these extraordinary elements allows today's scientist to follow in the footsteps of earliest chemists such as D. I. Mendeleev and colleagues. The gathered results with these new elements contribute to a generally better understanding of how so-called relativistic effects govern physicochemical properties of heavy elements.

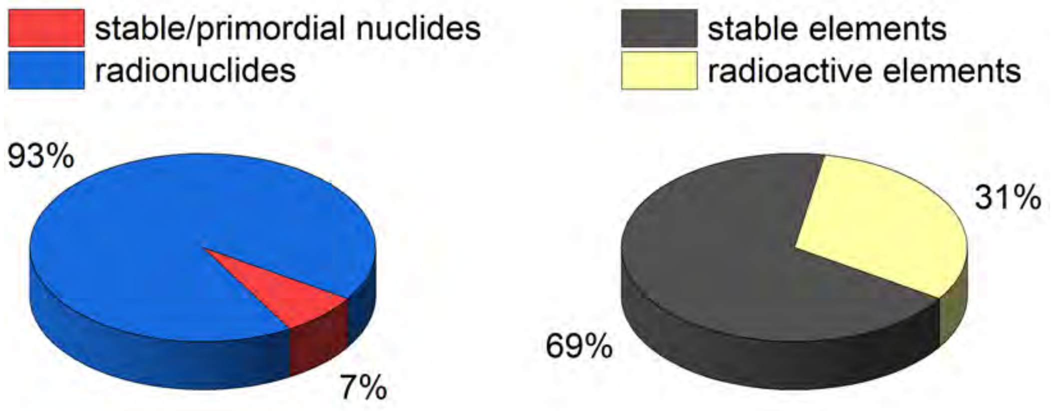

Figure 1: Pie charts of stable/primordial nuclides versus radionuclides (A) and stable elements versus radioelements (B).

The Atomic-Level Structure of Cementitious Calcium Aluminate Silicate Hydrate

P. Moutzouri[1]

[1]Institut des Sciences et Ingénierie Chimiques, EPFL Lausanne, CH-1015 Lausanne, Switzerland

A. Kunhi Mohamed,[2,6] P. Berruyer,[1] B. J. Walder,[1] J. Siramanont,[2,3] M. Harris,[2] M. Negroni,[1] S. C. Galmarini,[4] S. C. Parker,[5] K. L. Scrivener,[2] L. Emsley,[1] and P. Bowen[2]

[2] Laboratory of Construction Materials, Institut des Matériaux, EPFL Lausanne, CH-1015 Lausanne, Switzerland, [3] SCG CEMENT Co., Ltd., Saraburi 18260, Thailand, [4] Building Energy Materials and Components, EMPA, Switzerland, [5] Computational Solid State Chemistry Group, Department of Chemistry, University of Bath, UK, [6] Institute for Building Materials, Department of Civil, Environmental and Geomatic Engineering, ETH Zürich, CH-8073, Switzerland

Calcium silicate hydrate (C-S-H) is the main hydration product of ordinary Portland cement and has a layered calcium-silicate sheet structure with a disordered interlayer space that contains water molecules, hydroxyl groups and calcium ions. When present, aluminum can be incorporated into the C-S-H as aluminate species, forming calcium aluminate silicate hydrate (C-A-S-H). In C-A-S-H aluminum species are found having coordination numbers of four, five, and six. Here, using first principles calculations and advanced solid-state NMR techniques, we predict that at high Ca:Si and H_2O ratios, the stable coordination number of aluminum is six and that this aluminum species is incorporated into the bridging sites of the linear silicate chains. This is confirmed experimentally by one- and two-dimensional Dynamic Nuclear Polarization (DNP) enhanced ^{27}Al and ^{29}Si solid-state NMR experiments. In some of the highest field DNP MAS NMR experiments to date, we show that a narrow peak appearing at 5 ppm in the ^{27}Al NMR spectrum at 21.14 T can be assigned to the silicate-bridging $[AlO_2(OH)_4]^{5-}$ sites. A DNP enhanced 2D ^{27}Al/^{29}Si refocused dipolar INEPT MAS NMR experiment at 9.40 T was also used to correlate NMR signals from ^{27}Al nuclei that are less than ~4.3 Å from ^{29}Si (Figure 1). This experiment shows correlation of the 5 ppm ^{27}Al NMR signal with ^{29}Si NMR signals at -77 ppm. Using DFT shielding calculations we show that this ^{29}Si chemical shift is consistent with six-coordinate aluminate inserted as a bridge between silicate chains. We therefore answer the debated and long-standing question of the structural nature of aluminum in C-A-S-H.

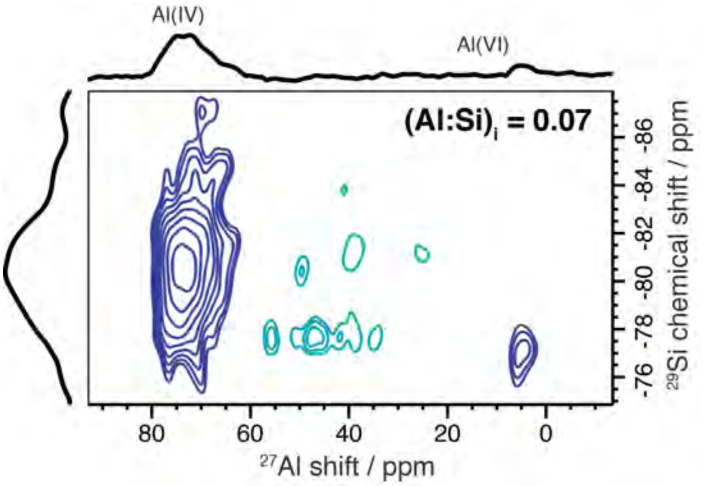

Figure 1: DNP enhanced two-dimensional {^{29}Si}^{27}Al refocused dipolar INEPT MAS spectrum acquired for a synthetic C-A-S-H sample (Ca:Si ratio of 2.0 and Al:Si ratio of 0.07) at 9.40 T, 100 K, and 10 kHz MAS.

Two-gap to single-gap superconducting transition in the $Ca_{1-x}Sr_xAlSi$ Solid Solution

D. I. Walicka[1], Z. Guguchia[2], J. Lago[3], O. Blacque[1], R. Lefèvre[1], K. Ma[1], F. O. von Rohr[1,4]*

[1]Department of Chemistry, University of Zurich, CH-8057 Zurich, Switzerland, [2]Laboratory for Muon Spin Spectroscopy, Paul Scherrer Institute, CH-5232 Villigen PSI, Switzerland, [3]Departamento de Química Inorgánica, Universidad del País Vasco, UVP/EHU, E-48080, Bilbao, Spain, [4]Department of Physics, University of Zurich, CH-8057 Zurich, Switzerland

The interest in compounds with AlB_2 structure type raised significantly after the discovery of the superconductivity in the layered compound MgB_2 with a critical temperature of $T_c = 39$ K [1]. CaAlSi and SrAlSi are ternary superconductors with the highest critical temperatures of $T_c = 8$ K, and 5 K, respectively, within this group [2]. They surprisingly differ in properties among each other, e.g. opposite pressure effect, although they have similar electronic and crystallographic structures [3].

Within this work we have synthesized and characterized the continuous $Ca_{1-x}Sr_xAlSi$ solid solution. We present an improved structural model for the parent compound CaAlSi and we show an evidence for the structural instability in CaAlSi to enhance the superconductivity across the solid solution. Furthermore, by means of muon-spin rotation experiments we prove that CaAlSi is a two-gap superconductor while SrAlSi is a single-gap superconductor, and that these two different electronic states are connected by a continuous transition.

[1] J. Nagamatsu, N. Nakagawa, T. Muranaka, Y. Zenitani, J. Akimitsu, *Nature*, **2001**, 410, 63–64.
[2] M. J. Evans, Y. Wu,V.F Kranak, N. Newman, A. Reller, F.J. Garcia-Garcia, U. Häussermann, *Physical Review B*, **2009**, 80, 064514.
[3] B. Lorenz, J. Cmaidalka, R.L. Meng, C.W. Chu, *Physical Review B*, **2003**, 68(1), 014512.

Silicon Oxycarbide as a Host Matrix of Choice to Stabilize Li-Ion Storage in Nanosized Alloying Elements

R. Dubey[1,3], P. Vallachira[2], F. Krumeich[1], G. Blugan[2], K. V. Kravchyk[1,3], T. Graule[2]*, M. V. Kovalenko[1,3]*

[1]Laboratory of Inorganic Chemistry, D-CHAB, ETH Zürich, [2]Laboratory for High Performance Ceramics, Empa, [3]Laboratory for Thin Films and Photovoltaics, Empa

The ever-increased demand in energy has led to a high necessity for innovative energy storage systems[1,2,3] with high energy densities, such as Li-ion batteries (LiBs). To maximize the anodic charge storage capacity of LiBs, alloying-type anode materials such as Sn and Sb have attracted considerable interest because of their high theoretical capacity of 992 and 660 mAh g^{-1} and a suitable lithiation/delithiation voltage window of 0.01–1.5 V *vs.* Li^+/Li. Recent advances in nanostructuring of the alloying-type anodes provide an effective way of mitigating the challenges of their volume expansion upon lithiation that severely hinder the cycling stability.[4] Besides, one of the prevailing approaches toward stabilization of such electrodes is the embedding of Sn or Sb in the form of nanoparticles (NPs) in a matrix. The matrix helps to buffer the volume changes, impart better electronic connectivity, and prevent particle aggregation upon lithiation/delithiation. In this context, polymer-derived ceramics, namely, silicon oxycarbide (SiOC), is an appealing candidate for stabilizing Sn and Sb inclusions. This matrix features a high Li-ion storage capacity ranging from 600 to 700 mAh g^{-1}, low volume expansion upon lithiation of about 7%, and high electronic conductivity. In this study, we report a facile synthesis of Sn[5] and Sb[6] NPs embedded in a SiOC matrix via the pyrolysis of a cross-linked preceramic polymer. The NPs are formed *in-situ* via a carbothermal reduction during the pyrolysis. We determined that a key element to obtain a homogeneous distribution of NPs in SiOC is the employment of precursors with compatible polarities, allowing for an intimate blending of the functionalized polysiloxanes with the Sn or Sb precursors. This approach proved to be effective for buffering volume changes while retaining practical energy densities and high rate capabilities. For instance, SiOC/Sn nanocomposite exhibited a high rate capability, delivering a high capacity of 553 mAh g^{-1} at a current density of 2232 mA g^{-1} (≈ 6C for a graphite anode). Additionally, the electrochemical performance of SiOC was assessed in full cell configuration using areal capacities of 1.3 mAh cm^{-2} being relevant for high-power industrial applications. The mechanism of Sn lithiation in SiOC was evaluated by *in-situ* powder X-ray diffraction.

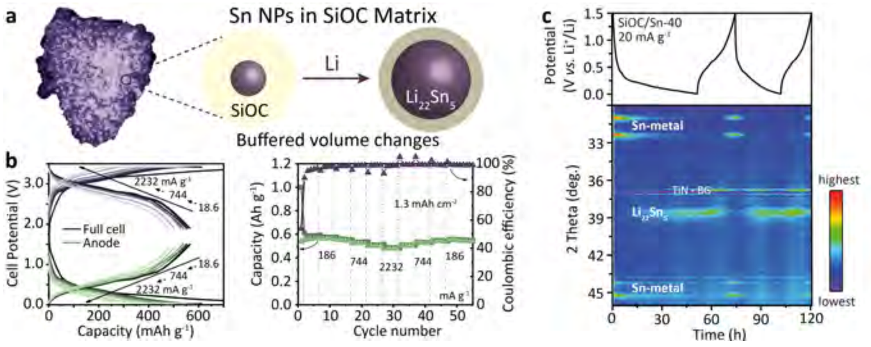

[1] R. Dubey et al. *ACS Applied Mater. Interfaces* **2019**, *11*, 17686.
[2] K. Kravchyk, R. Dubey et al. *Sci. Rep.* **2019**, 9, 1-8.
[3] R. Dubey, et al. *ACS Applied Mater. Interfaces* **2019**, *11*, 39902.
[4] M. Nasir, et al. *Adv. Energy Mater.* **2016**, *6*, 1600374.
[5] R. Dubey, et al. *Adv. Sci.* **2019**, *6*, 1901220.
[6] R. Dubey et al. **2020**, *in revision.*

Improvement of a Single-Ion Magnet Performance Using the Surface Organometallic Chemistry Approach

M. D. Korzyński[1], Z. J. Berkson[1], O. Cador[2], B. Le Guennic[2], C. Copéret[1]*

[1]Department of Chemistry and Applied Biosciences, ETH Zürich, Vladimir-Prelog-Weg 1-5/10, 8093 Zürich, Switzerland, [2]Institut des Sciences Chimiques de Rennes, Université de Rennes 1, 35042 Rennes, France

Development of molecules exhibiting slow relaxation of magnetization has been an active area of research for more than 25 years.[1] These single-molecule magnets (SMMs) hold promise for high density information storage, quantum computing and spintronics applications. More recent focusing on lanthanide-based single ion magnets (SIMs) has been a particularly worthwhile endeavor as it led not only to discovery of the best performing SMMs to date, but also to further elaboration of organolanthanide chemistry. The latter stems from the fact that classical organometallic ligands such as cyclopentadienide and cyclooctatetraenide (COT) align well with the theoretical design principles for achieving superior SIMs.

Heterogenization of these molecular complexes has received much less attention in the literature, despite its paramount importance from the perspective of practical implementation in devices.[2] Most of the work done to date explored the non-covalent deposition of known SMMs on metal surfaces, but such immobilization strategy typically leads to a sharp decrease of magnetic performance presumably due to a perturbation of the desired metal geometry/electronics and a misalignment of magnetization easy-axes upon grafting. While direct covalent attachment of SMM could in principle provide more control over directionality, it has so far been hardly explored.

In this contribution we demonstrate that covalent grafting of an established COT-based SIM on the surface of partially dehydroxylated silica through surface organometallic chemistry (SOMC)[3] can significantly improve its magnetic performance. This approach allows us not only to maintain hysteretic behavior of the parent system, but also provide magnetic site separation and increase the relaxation time by two orders of magnitude. With the preeminence of organolanthanide systems our approach holds promise for broader applicability in the field.

Acknowledgements:
The authors acknowledge ERC MULTIPROSMM project (grant no. 725184); MDK would like to thank ETH Zurich Postdoctoral Fellowships program (FEL-23 19-1).

[1] Layfield, R. A. *Organometallics*, **2014**, *33*, 1084.
[2] Holmberg, R. J.; Murugesu, M. *J. Mater. Chem. C*, **2015**, *3*, 11986.
[3] Copéret, C.; Comas-Vives, A.; Conley, M. P.; Estes, D.; Fedorov, A.; Mougel, V.; Nagae, H.; Núñez- Zarur, F.; Zhizhko, P. A. *Chem. Rev.*, **2016**, *116*, 323.

Nuclear Quadrupole Resonance of multinary $FA_{1-x}Cs_xPbI_{3-y}Br_y$ Perovskites

M. Aebli[1,2], M. V. Kovalenko[1,2]*

[1]Department of Chemistry and Applied Biosciences, ETH Zürich, Vladimir-Prelog-Weg 1-5,
CH-8093, Switzerland., [2]Empa-Swiss Federal Laboratories for Materials Science and Technology,
Dübendorf, Überlandstrasse 129, CH-8600, Switzerland.

Formamidinium (FA)-based hybrid lead iodide perovskites ($FAPbX_3$, X=I or Br/I) have recently led to significant improvements in the performance of perovskite photovoltaics. One of the remaining major hurdles is the instability of α-$FAPbI_3$, which undergoes a phase transition from the desired three-dimensional cubic perovskite phase to a non-perovskite one-dimensional hexagonal lattice. Partial substitution of FA with Cs and, concomitantly, iodide with bromide is known to stabilize the material's cubic perovskite structure, as shown by X-ray diffraction. Nuclear quadrupole resonance (NQR) has been reported to resolve structural changes with accuracies commensurate with synchrotron X-ray diffraction and scattering.[1] We report the ^{127}I NQR spectra of $FA_{1-x}Cs_xPbI_{3-y}Br_y$ (x=0-0.1, y=0-3) showing not only the averaged but also the local iodide structures. Upon ion replacement, massive line broadening and new species can be observed, which could be assigned to various coordination environments. These findings showcase the great potential of halide NQR for characterizing perovskite-based materials.

[1] L. Piveteau, *et al.,* “Bulk and Nanocrystalline Cesium Lead Halide Perovskites as seen by Halide Magnetic Resonance”, *ACS Central Science,* **2020**, accepted.

Alkoxide-Mediated Metal Halogen Exchange Reactions

L. J. Bole[1], N. R. Judge[2], E. Hevia[2]*

[1]University of Bern , [2]University of Bern

Classical lithium-halogen exchange reactions are one of the cornerstone synthetic protocols in organometallic chemistry. Although indispensable, these transformations suffer drawbacks in the essential use of cryogenic temperatures and ethereal solvents, alongside the problem of limited functional group tolerance, due to the highly reactive nature of the organolithium reagents employed.[1] Combining the efficiency of organolithiums with the selectivity of a lower polarity organometallic species such as R_2Mg or R_2Zn (R = alkyl), permits milder conditions and broader compatibility with more elaborate functional groups.[2] Recent advances have shown that replacing RLi with LiOR' (R' = $CH_2CH(CH_2)C_4H_9$ or $C_2H_4(NMe)C_2H_4(NMe_2)$) leads to efficient Mg-Br and Zn-Br exchange reactions at room temperature in the industrially friendly solvent toluene.[3] Nevertheless, the rationale behind these enhanced reactivities and the exact effect of LiOR still remain to be established.

Shedding light into the hidden constitution of these multimetallic systems, this work provides the first structural and spectroscopic evidence for the formation of heteroleptic mixed-metal exchange reagents and the metallated intermediates that they give rise to. The key effects that donor solvents and functional group substituents on the aromatic substrate play in controlling the efficiency and selectivity of the exchange reactions will also be presented.

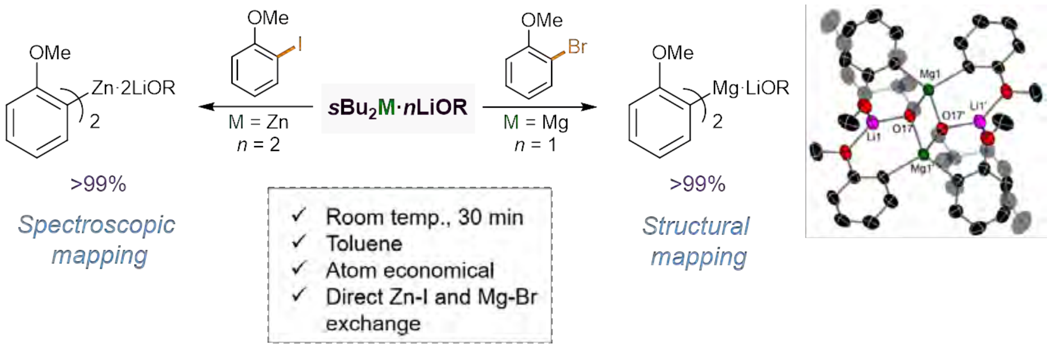

- ✓ Room temp., 30 min
- ✓ Toluene
- ✓ Atom economical
- ✓ Direct Zn-I and Mg-Br exchange

[1] *Organometallics Third Ed.* (Elschenbroich C.), Wiley-VCH, Marburg, **2016**.
[2] T. Furayama, M. Yonehara, S. Arimoto, M. Kobayashi, Y. Matsumoto, M. Uchiyama, *Chem. Eur. J.*, 2008, **14**, 10348; T. D. Bluemke, W. Clegg, P. García-Alvarez, A. R. Kennedy, K. Koszinowski, M. D. McCall, L. Russo, E. Hevia, *Chem. Sci.*, **2014**, 5, 3552.
[3] D. S. Ziegler, K. Karaghiosoff, P. Knochel, *Angew. Chem. Int. Ed.*, **2018**, 57, 6701; M. Balkenhohl, D. S. Ziegler, A. Desaintjean, L. J. Bole, A. R. Kennedy, E. Hevia P. Knochel, *Angew. Chem. Int. Ed.*, **2019**, 58, 12898.

The origin of trap-states in monodisperse formamidinium tin iodide nanocrystals

D. N. Dirin[1,2], A. Vivani[1,3], M. I. Bodnarchuk[2], M. Aebli[1], I. Cherniukh[1,2], A. Guagliardi[3,4], M. V. Kovalenko[1,2]*

[1]Department of Chemistry and Applied Biosciences, ETH Zürich, [2]Laboratory for Thin Films and Photovoltaics, Empa , [3]University of Insubria, Department of Science and High Technology, [4] Institute of Crystallography, Italy

Over the last nine years, lead halide perovskites have been a subject of continuous interest due to a combination of several unique properties, particularly long diffusion length of carriers, optoelectronic tolerance to intrinsic defects, and highly dynamic crystal lattice. These materials have exhibited the well-recognized success towards application in solar cells, light-emitting devices, and high-energy radiation detectors. There was also significant progress in the understanding of the origin of their unique optoelectronic properties on both bulk- and nano-scale levels. This new understanding indicates that finding an alternative lead-free material with similar optoelectronic properties among other, non-group-14 metal halides can be very challenging if possible at all. On the other hand, recent advances in metal halide perovskite photovoltaics indicate that the closest analog to lead halide perovskites, namely formamidinium tin iodide, could exhibit similarly exciting performance if synthesized with a low number of trap states. The main challenge with this material relates to the easiness of trap states generation during the processing of this material, which is often ascribed to the oxidation of Sn(II) to Sn(IV). In this work we present a new synthesis of colloidal formamidinium tin iodide nanocrystals with a high degree of monodispersity and show that such oxidation is not the only pathway of formamidinium tin iodide degradation and low photoluminescence quantum yield.

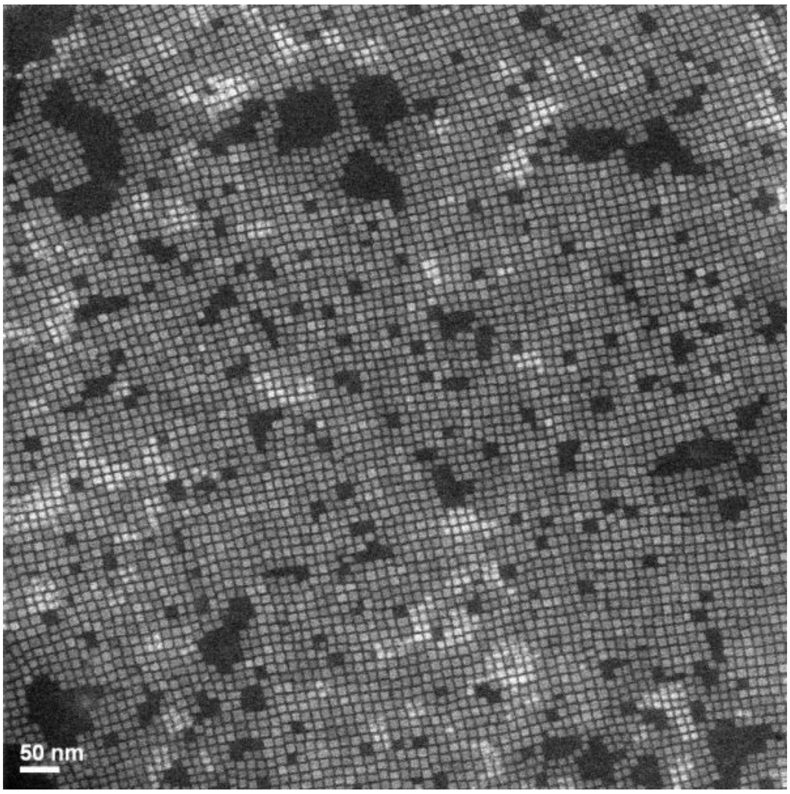

Exploring the chemical scope of light activated protein conjugation using desferrioxamine B derivatives

D. F. Earley[1], A. Guillou[1], J. P. Holland[2]*

[1]University of Zurich, Department of Chemistry, [2]University of Zurich, Department of Chemistry, Zurich

Due to their unique structure, function, high-affinity and target specificity, protein conjugates have fast become essential tools in medical imaging. For example, in the clinic, monoclonal antibodies (mAbs) functionalised with metal-binding chelates such as desferrioxamine B (DFO), and radiolabelled with zirconium-89 (^{89}Zr-mAbs) provide sophisticated, rationally-designed, protein-based radiopharmaceuticals for use in positron emission tomography (PET). In this context, the preparation of radiolabelled protein conjugates requires the formation of a new covalent bond between the protein and the ligand, which must be achieved without disrupting the structural and biological properties of the target protein. Photochemistry offers new synthetic routes toward protein conjugates including ^{89}Zr-mAbs, through the use of photoactivatable radio-metal binding chelates. Here, we report the synthesis of a series of photoactivatable DFO-derivatives functionalised with a variety of photoactivatable groups including aryl azides, diazarines, and benzophenones, to explore the chemical scope of photoactivated protein conjugation reactions via several distinct mechanisms, including ketenimines, stabilised singlet nitrenes, carbenes and radicals. We evaluate their use for the *photoradiosynthesis* of ^{89}Zr-labelled protein conjugates and demonstrate radiochemical yields up to 72.9±1.9 % (using *p*-ArN$_3$-PEG$_3$-DFO).

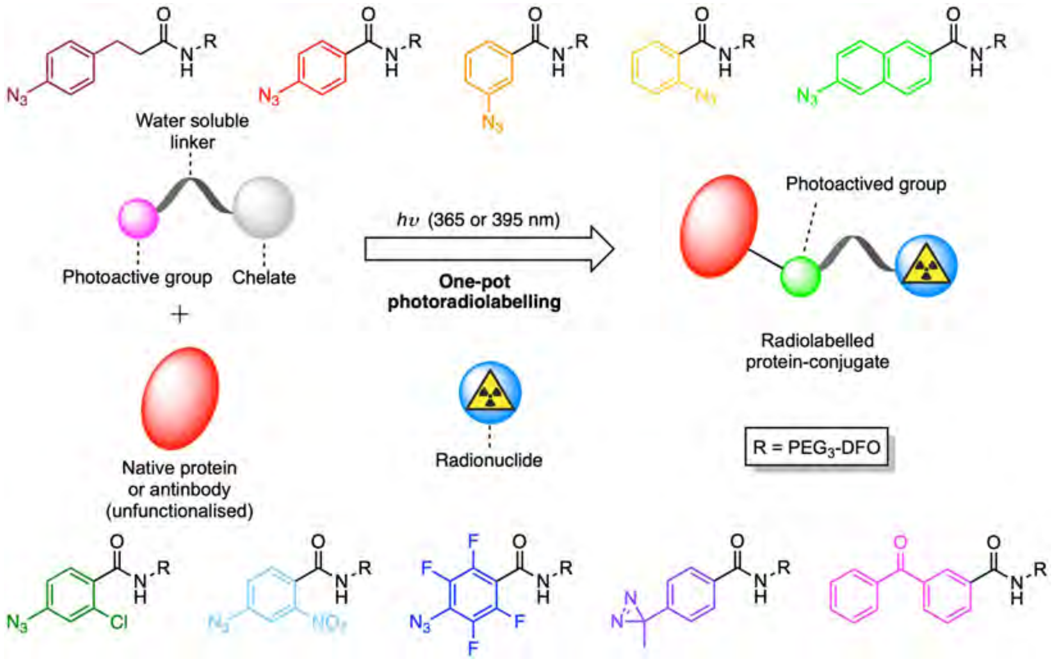

Reversible Cyclometallation of Aryl-Pya Iridium Complexes

A. Farre[1], M. Albrecht[1]*

[1]Department für Chemie und Biochemie, Universität Bern

Classically, ligands of homogeneous catalysts have a set of intrinsic and static electronic properties that stabilize the metal center and impart specific activity and selectivity.[1] In the last decades, the development of functional ligand motives such as Noyori's diamine ligand[2] has become a major effort in the field of organometallic chemistry. As an alternative strategy, ligands with flexible donor properties are highly attractive for stabilizing metals in different oxidation state, *e.g.* on a catalytic cycle.[3] Pyridylideneamides (PYA) are such electronically flexible ligands that can modulate the electron donation by coordinating to the metal center as a π-acidic imine, or as a π-basic zwitterionic pyridinium amide. Herein, we present a set of aryl-PYA iridium complexes that exhibit reversible cyclometallation indicated by deuterium incorporation on the aryl moiety (see Figure 1). This process is enhanced with the introduction of electron donating substituents on the aryl ring.

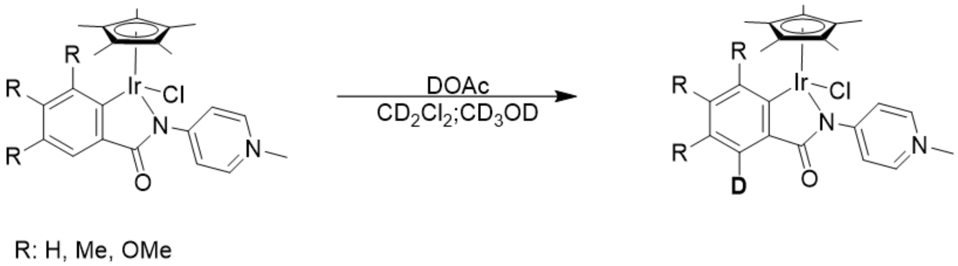

Figure 1. Deuterium incorporation on the aryl moiety

[1] John F. Hartwig, *Organotransition Metal Chemistry*, University Science Books, Mill Hill Valley, California, **2010**.
[2] Ryoji Noyori, Takeshi Okhuma, *Angew. Chem. Int. Ed*. **2001**, 40, 40-73.
[3] Miquel Navarro, Mo Li, Helge Müller-Bunz, Stefan Bernhard, Martin Albrecht, *Chem. Eur.J.* **2016**, 22, 6740-6745.

The introduction of ^{161}Tb to the clinic through the Good Manufacturing Practice compliant production of ^{161}Tb-DOTATOC

C. Favaretto[1,4], Z. Talip[1], P. V. Grundler[1], S. Geistlich[1], S. Landolt[1], J. R. Zeevaart[2], U. Köster[3], R. Schibli[1,4], N. P. van der Meulen[1]*

[1]Center for Radiopharmaceutical Sciences ETH-PSI-US, [2]Radiochemistry NECSA, [3]Institut Laue-Langevin, Grenoble, France, [4]Department of Chemistry and Applied Biosciences ETH, [5]Laboratory of Radiochemistry ETH-PSI-US

The radionuclide ^{161}Tb ($T_{1/2}$ = 6.95 d [1]) shows similar decay characteristics and chemical behavior to ^{177}Lu, which is currently regarded as the “gold standard” of targeted radionuclide therapy. However, on a preclinical level, ^{161}Tb has proven to be superior as a result of its co-emission of conversion and Auger electrons [2,3]. The aim of this study was to demonstrate the possibility to produce ^{161}Tb with a robust process to ensure reproducible quality and quantity of product for its introduction to the clinic. In particular, efforts were put into the characterization of the novel radionuclide and the development of a protocol towards Good Manufacturing Practice (GMP)-compliant production of ^{161}Tb-DOTATOC.

^{161}Tb production was carried out with a previously-established method by neutron irradiation of enriched ^{160}Gd oxide targets, using the $^{160}\mathrm{Gd}(n,\gamma)^{161}\mathrm{Gd}\rightarrow^{161}\mathrm{Tb}$ nuclear reaction [4]. No-carrier-added (n.c.a.) ^{161}Tb was obtained after its separation from ^{160}Gd target material using cation exchange chromatography and extraction chromatography. The process led to a production yield in the range of 8-20 GBq ^{161}Tb at concentrations of 4-19 MBq/µL. The quality of the labeling solution obtained was evaluated: in particular, pH, radionuclidic purity, radiochemical purity and the limit of endotoxins of the $^{161}\mathrm{TbCl}_3$ labeling solution were assessed, in order to validate the characteristics necessary for its introduction to a clinical setting. Moreover, using this labeling solution, it was possible to carry out a promising preliminary study for the production of ^{161}Tb-DOTATOC compliant with the principles of Good Manufacturing Practice (GMP). ^{161}Tb-DOTATOC was synthesized, for the first time using a modular automated system, as a product with specifications and activity levels suitable for clinical use, i.e. from 1.0 to 7.4 GBq in 20 mL at 53 MBq/nmol molar activity. The production yield was demonstrated to be >85% and the product stable over a 24 hours period. High-performance liquid chromatography and gas chromatography techniques were used for quality control. A suitable method was established for both the techniques and the range and linearity of the detection were assessed, respectively. A matrix-based bubble point test for the control of the sterilizing filter after the vial filling process was also developed.

In conclusion, high yields of $^{161}\mathrm{TbCl}_3$ were produced in a quantity and quality suitable for potential clinical applications. Based on the quality of the product, a GMP-compliant production and quality control process of ^{161}Tb-DOTATOC was preliminarily evaluated. Further studies to validate the production and quality control of the whole process will be performed and the documentation prepared for submission to the regulatory authorities.

[1] M. Teresa Durán *et al.*, *Applied Radiation and Isotopes*, **2020**, 159:109085, 1–9.
[2] Cristina Müller *et al.*, *European Journal of Nuclear Medicine and Molecular Imaging*, **2014**, 41:3, 476–485.
[3] Cristina Müller *et al.*, *European Journal of Nuclear Medicine and Molecular Imaging*, **2019**, 46:9, 1919–1930.
[4] Nadezda Gracheva *et al.*, *EJNMMI Radiopharmacy and Chemistry*, **2019**, 4:12, 1–16.

Development of the matched pair Sc-44/Sc-47 for diagnosis and therapy

P. V. Grundler[1], R. Hasler[1], C. Favaretto[1,4], Z. Talip[1], G. Dellepiane[2], T. S. Carzaniga[2], S. Braccini[2], U. Köster[3], C. Müller[1], N. P. van der Meulen[1,5]*

[1]Center for Radiopharmaceutical Sciences ETH-PSI-USZ, Paul Scherrer Institute, Villigen-PSI, Switzerland, [2]Albert Einstein Center for Fundamental Physics, Laboratory of High Energy Physics, University of Bern, Bern, Switzerland, [3]Institut Laue-Langevin, Grenoble, France, [4]Department of Chemistry and Applied Biosciences, ETH Zurich, Zurich, Switzerland, [5]Laboratory of Radiochemistry, Paul Scherrer Institute, Villigen-PSI, Switzerland

In nuclear medicine, the concept of theragnostics implies the use of two radionuclides with very similar chemical properties, ideally from the same elements, but with emission of different types of radiation, suited for either imaging or therapy - rarely for both. Scandium can provide such a matched pair with its radioisotopes ^{44}Sc and ^{47}Sc [1].

The favourable decay properties of ^{44}Sc ($T_{1/2}$ = 4.04 h, I_{β^+} = 94%, E_{β^+av} = 632 keV) [2, 3] for cancer diagnosis using positron emission tomography (PET) makes it a promising candidate for application in nuclear medicine [4]. On the other hand, ^{47}Sc is a low-energy β^--emitter ($T_{1/2}$ = 3.35 d; E_{β^-av} = 162 keV) which is potentially useful for radionuclide tumour therapy similar to the clinically well-established ^{177}Lu ($T_{1/2}$ = 6.65 d; E_{β^-av} = 134 keV) [5].

To this end, the production of ^{44}Sc from a $CaCO_3$ target via the ^{44}Ca(p,n)^{44}Sc nuclear reaction using a cyclotron was developed [6]. Natural Ca can be used, but enriched ^{44}Ca increases the yield and reduces the side products. Recently, this approach has been improved for production with a medical cyclotron [7, 8]. On the other hand no carrier added ^{47}Sc is produced at a neutron source via the ^{46}Ca(n,g)^{47}Ca nuclear reaction [1, 5] followed by β^- decay of the intermediary product ^{47}Ca ($T_{1/2}$ = 4.54 d) to ^{47}Sc. In both cases, the recovery of the Sc from the Ca target is easily achieved by dissolving the target in HNO_3 and using a DGA extraction resin.

The products from both production routes were successfully used for radiolabelling, biodistribution and in vivo imaging or pre-clinical therapeutic studies, thus, highlighting the potential of this matched pair.

[1] Müller, C.; Bunka, M.; Haller, S.; Köster, U.; Groehn, V.; Bernhardt, P.; van der Meulen, N.; Türler, A.; Schibli, R., *Journal of Nuclear Medicine* **2014,** 55 (10), 1658-1664.
[2] García-Toraño, E.; Peyrés, V.; Roteta, M.; Sánchez-Cabezudo, A. I.; Romero, E.; Martínez Ortega, A., *Applied Radiation and Isotopes* **2016,** 109, 314-318.
[3] NuDat 2.7. https://www.nndc.bnl.gov/nudat2/.
[4] Rösch, F.; Baum, R. P., *Dalton Transactions* **2011,** 40 (23), 6104-6111.
[5] Domnanich, K. A.; Müller, C.; Benešová, M.; Dressler, R.; Haller, S.; Köster, U.; Ponsard, B.; Schibli, R.; Türler, A.; van der Meulen, N. P., *EJNMMI Radiopharmacy and Chemistry* **2017,** 2 (1), 5.
[6] van der Meulen, N. P.; Bunka, M.; Domnanich, K. A.; Müller, C.; Haller, S.; Vermeulen, C.; Türler, A.; Schibli, R., *Nuclear Medicine and Biology* **2015,** 42 (9), 745-751.
[7] Braccini, S.; Belver-Aguilar, C.; Carzaniga, T. S.; Dellepiane, G.; Haeffner, P.; Scampoli, P. In *Novel Irradiation Methods for Theranostic Radioisotope Production With Solid Targets at the Bern Medical Cyclotron*, International Conference on Cyclotrons and their Applications, Cape Town, South Africa, 2019/05; Schaa, V. R. W., Ed. JACoW Publishing: Cape Town, South Africa, 2019; pp 128-132.
[8] van der Meulen, N.P., et al., in preparation

Functionalized single-layer graphene for carbon capture

K. Hsu[1]

[1]Laboratory of Advanced Separations (LAS), Lausanne

Carbon capture by membranes separation from flue has attracted much attention in reducing greenhouse gas emissions due to the modularity and ease of retrofitting membranes. As it is operated with low energy requirements and without generating chemical waste, membranes separation is an environmental-friendly route. Especially, molecular-sieving membranes with permeance over 1000 GPU with a CO_2/N_2 selectivity exceeding 20 significantly improve the energy efficiency of separation[1].

Ideally, high-performance molecular-sieving membranes should have CO_2 selective transport channel, high porosity, and a small diffusion path-length. Single-layer graphene (SLG) is highly promising for this but has an impermeable lattice. A precise etching of sub-angstrom pores in graphene is regarded as a bottleneck for the development of SLG membranes. The pore generation in the graphene lattice involves nucleation and growth happening simultaneously, leading a broad pore size distribution (PSD). A narrow PSD allows high resolution of molecular-sieving, like separating only 0.3 Å difference between CO_2 and N_2. To fulfill this, decoupling nucleation and growth of pores is one of the most promising ways[2]. Recently, we developed precise ozone-led gasification chemistry that generates a high number of pores followed by exclusive pore growth; Tunable ozone concentration determines pore nucleation and pore growth. By this new approach, gas-sieving nanoporous single-layer graphene membranes, with record-high CO_2 permeance and molecular sieving resolution down to 0.3 Å, has been achieved.

To further enhance the gas selectivity, functionalizing a CO_2-philic layer on porous graphene is a promising approach. Polymer-functionalized nanoporous graphene (SPONG) membranes offer a platform for selectively adsorbing CO_2, increasing the separation factor[3]. The epoxy groups on graphene are the grafting site for amine-terminated polymers via the ring-opening chemistry. Such polymeric layers on graphene can be further engineered, by swelling of polymeric chains. Impregnation of poly(ethylene glycol)-dimethyl-ether (PEGDE) into polyethylenimine (PEI) network increases the free-volume between the polymer chain by altering the hydrogen-bonding between polymer chain network.

Finally, a novel gasification reactor has been developed which allows for improved control over the etching kinetics (reaction time, temperature, concentration). The rapid sample heating (5-10 milliseconds) in this gasification reactor offers potential for studying ozone etching mechanisms, like chemisorption, clustering, and gasification.

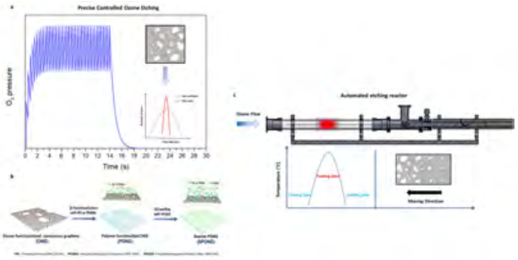

[1] Merkel, T.C., et al., Journal of Membrane Science, **2010**, 359, 126-139.
[2]Shiqi Huang, L.F.V., Shaoxian Li, Deepu J. Babu, Mohammad Tohidi Vahdat, Emad Oveisi, Kumar Varoon Agrawal, submitted.
[3]He, G., et al., Energy & Environmental Science, **2019**, 12, 3305-3312.

Incorporating vacancy defects in single-layer graphene lattice with a sub-1-Å resolution

S. Huang[1], K. V. Agrawal[1]*

[1]Laboratory of Advanced Separations (LAS), École Polytechnique Fédérale de Lausanne (EPFL)

Graphene, as the thinnest molecular barrier with the extraordinary mechanical and thermal stability, can be extremely attractive porous interface to realize energy-efficient molecular sieving. Nanopore with suitable aperture size can be incorporated in the graphene lattice to selectivity allow the passage of specific molecules.[1-3] However, the state-of-the-art carbon etching chemistries are not easy to control at the atomic scale. As a result, incorporation of a narrow enough pore-size-distribution that is needed for the separation of similarly-sized gas molecules (CO_2, N_2, CH_4) has been elusive.

In this talk, I will discuss a novel ozone-based carbon gasification chemistry applied in the custom-made millisecond gasification reactor (MGR), which controls the etching kinetics (vacancy nucleation, and pore expansion) to a few milliseconds.[4] Rapid and controllable etching of the graphene lattice could be achieved by introducing a millisecond pulse of ozone at moderately high temperature (250-290 ºC), followed by synchronous spontaneous purging of ozone. Optimized ozone dose led to attractive pore density (10^{12} cm^{-2}), while high-resolution transmission electron microscopy and low-temperature scanning tunneling microscopy study revealed that most of the nanopores were smaller than those created by missing 20 carbon atoms. Relative transport rates of H_2, CO_2, O_2, N_2, and CH_4, with the kinetic diameter in the range of 0.289 – 0.38 nm, were used as characterize the gas sieving performance. Overall, these nanopores could sieve CO_2 (kinetic diameter of 3.3 Å) and O_2 (kinetic diameter of 3.46 Å) from N_2 (kinetic diameter 3.64 Å), with CO2/O2 and CO2/N2 selectivities of 13 and 20, respectively, corresponding to a molecular sieving resolution of 0.2 Å. Furthermore, the slow expansion of vacancy-defects with oxygen exposure at 200 ºC could shift the molecular cut-off by 0.1 Å. The membrane reached CO_2/N_2 selectivity of 21.7 with a record-high CO_2 permeance of 11850 GPU. The millisecond gasification chemistry discussed here will generate new avenues for material chemistry in the context of controlled formation of defects in two-dimensional materials.

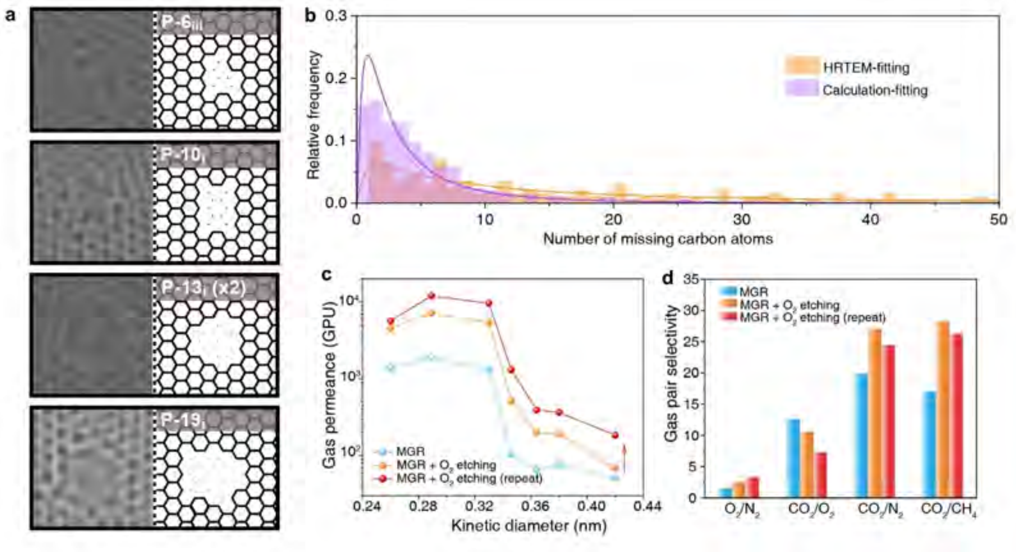

[1] Wang, L. and Karnik, R. *Nature Nanotechnology* **2017**, 12, 509–522.
[2] Huang, S. and Agrawal, K. V. *Nature Communications* **2018**, 9, 1–11.
[3] Zhao, J. and Agrawal, K. V. *Science Advances* **2019**, 5, eaav1851.
[4] Huang, S. and Agrawal, K. V. Submitted.

DNA-ferrocene as two-step-mechanophore

E. JEAN-PIERRE[1], E. JANETT[1], C. Bochet[1], K. M. Fromm[1]*

[1]Department of Chemistry, University of Fribourg,

Depuis de nombreuses années, les chercheurs cherchent aux complexes de type sandwich qui peuvent être utilisés dans divers domaines comme la catalyse, l'électrochimie, les applications agrochimiques ou pour la production de produits pharmaceutiques et d'arômes. [1, 2] Récemment, nous avons montré que le ferrocène peut être utilisé comme mécanophore dans les polymères, donc comme point de rupture préférentiel dans le poly méthylacrylate et le polyuréthane. [3]

Nous avons maintenant introduit une fonctionnalité supplémentaire en associant les fragments ferrocènes via un linker [4] à un duplex d'ADN. L'incorporation d'une telle entité dans un polymère devrait donner naissance à un mécanophore en deux étapes [5] (figure 1) dans laquelle les liaisons H de l'ADN, puis le complexe sandwich sont clivés à mesurer qu'une force s 'accumulent est exercée. Les mésappariements introduits dans l'appariement d'ADN ont une influence sur la résistance mécanique du mécanophore.

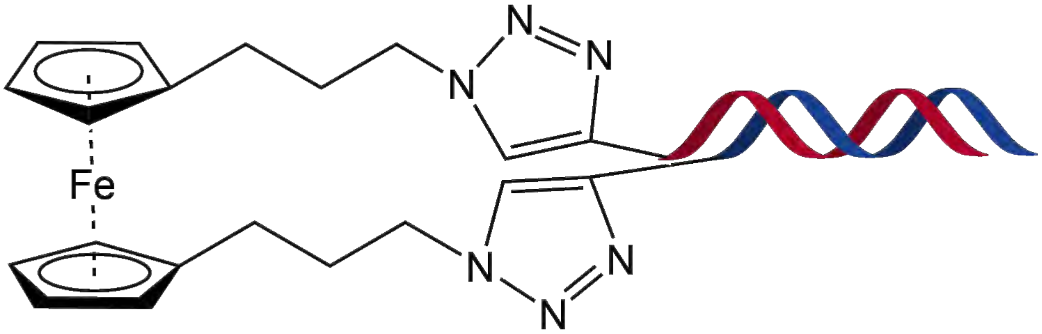

[1] TJ Colacot, Nouvelle-Écosse Hosmane, *Z. Anorg. Allg. Chem.,* **2005** , 631, 2659-2668.
[2] C. Sui, Y. Zhou, M. Wang, H. Yin, P. Wang, S. Ai, *Sensors and Actuators B.* , **2018** , 514-521.
[3] M. Di Giannantonio, MA Ayer, E. Vester-Sesto, M. Lattuada, C. Weder, KM Fromm, *Angew.Chem.Int. Ed.* , **2018** , *57* , 11445 –11450.
[4] R. Claus, JP Lewtak, TJ Muller, JC Swarts, *J. Organomet. Chem.* , **2013** , *740* , 61-69.
[5] J. Li, C. Nagamani, JS Moore, *Acc. Chem. Res* ., **2015** , 48 (8), 2181-2190.

Carbon Dioxide Reductive Disproportionation Driven by Electron-Rich f-Elements Complexes Supported by Heptadentate Non-Innocent Ligands

N. Jori[1], M. Falcone[1], D. Toniolo[1], R. Scopelliti[1], M. Mazzanti[1]*

[1]Institut des Sciences et Ingénierie Chimiques, EPFL

The use of non-innocent redox ligands in the synthesis of coordination compounds is gaining considerable attention in recent years. The cooperativity between the metal center and the ligands, which can act as electron reservoirs, [1] can allow their involvement in multi-electron redox processes. Uranium commonly engages in monoelectron transfer processes, therefore the possibility of storing extra electrons in the ligand framework can open new pathways in its redox activity towards the small molecule activation.

Polydentate Schiff bases were shown more than two decades ago to act as redox active ligands, through the reversible formation and cleavage of C-C bonds. However, the use of these ligands to facilitate electron transfer in f elements complexes remains significantly less explored than for the transition metals. [2]

We will present the synthesis, structural properties and reactivity of f-elements complexes with the heptadentate Trensal ligand. These complexes are not only able to store up to 4 electrons in the ligand framework, but also are capable of insert or reduce CO_2 with concomitant formation of carbonate. [3]

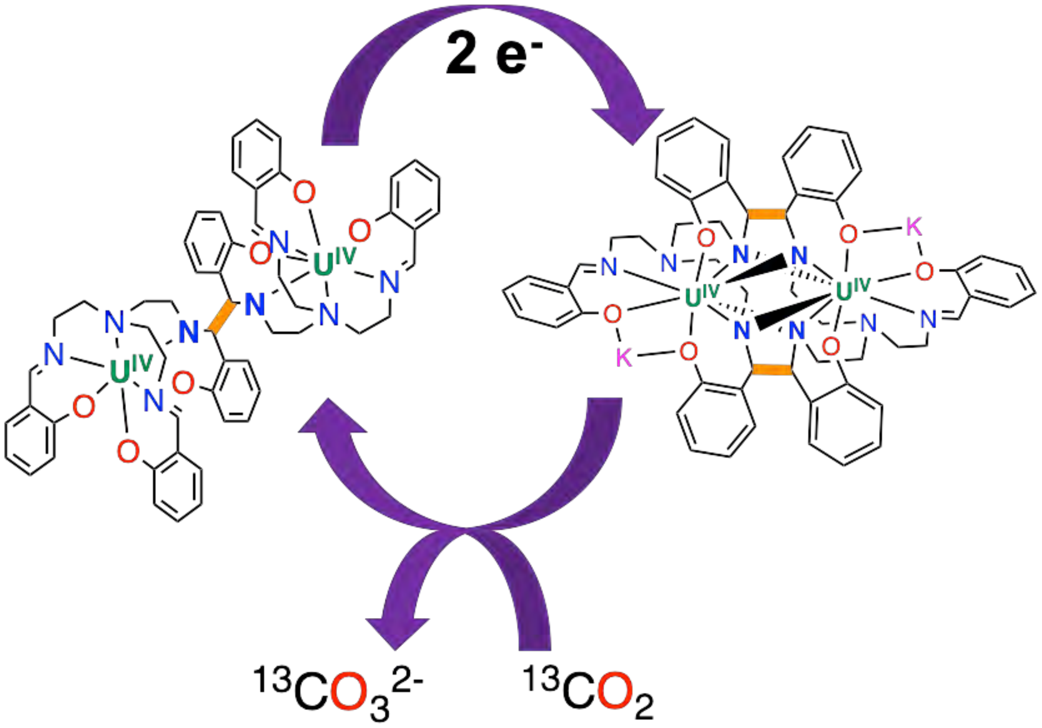

[1] Volodymyr Lyaskovskyy, Bas de Bruin, ACS Catalysis, **2012,** *2* (2), 270-279
[2] Julie Andrez, Valentin Guidal, Rosario Scopelliti, Jacques Pécaut, Serge Gambarelli, Marinella Mazzanti, *J. Am. Chem. Soc.,* **2017**, 139, 25, 8628-8638
[3] Nadir Jori, Marta Falcone, Rosario Scopelliti, , Marinella Mazzanti, *Organometallics* **2020**, 39, 9, 1590–1601

Shedding light on Lithium-Alkoxide Mediated Magnesium-Bromine Exchange Reaction.

N. R. Judge[1]

[1]University of Bern

Metal-halogen exchange reactions constitute one of the most powerful methodologies for the functionalisation of aromatic halides. While conventional Grignard reagents are typically sluggish to react with bromoarenes, Turbo Grignard reagents (RMgCl.LiCl) have emerged as efficient and selective systems capable of promoting Mg-bromine exchange under mild reaction conditions.[1,2] More recently a new type of mixed lithium-magnesium reagents, namely $s\mathrm{Bu_2Mg.2LiOR}$ (R = 2-ethylhexyl), has been introduced which offers even more enhanced reactivities and greater functional group tolerance as well as being compatible with the use of toluene as a solvent.[3] Nevertheless the reasons behind these unique behaviours still remain unknown.

Filling this gap in the knowledge, this work presents the first structural and spectroscopic insights into the hidden constitution of these bimetallic systems and their abilities to perform selective Mg-Br exchange (see Figure). The influence that directing groups present on the aromatic substrate and donor solvents play in these Mg-Br interconversions will also be presented.

[1] A. Krasovskiy and P. Knochel, *Angew. Chem. Int. Ed.*, **2004**, *43*, 3333.
[2] Bao, R. L.-Y.; Zhao, R.; Shi, L. *Chem. Commun*. **2015**, *51,* 6884.
[3] D. S. Ziegler, K. Karaghiosoff, P. Knochel, *Angew. Chem. Int. Ed.* **2018**, *57*, 6701.

Scale-up of gas-sieving nanoporous single-layer graphene membrane[1]

W. Lee[1], K. V. Agrawal[2]

[1]Laboratory of Advanced Separations (LAS), Institute of Chemical Sciences & Engineering (ISIC), École Polytechnique Fédérale de Lausanne (EPFL), [2]Laboratory of Advanced Separations (LAS), EPFL

Nanoporous single-layer graphene (NSLG) membranes are promising for gas separation, capable of yielding large yet molecule-selective permeance.[2] However, the scale-up of such NSLG membrane remains challenging. Typically, cracks and tears are introduced into the suspended graphene during the membrane fabrication, and dominate the overall gas transport.[3] Herein, we will demonstrate the fabrication of centimeter-scale crack-free gas-sieving NSLG membranes, on a low-cost macroporous support, by mechanically reinforcing the graphene film with a two-layer composite carbon film that prevents crack generation and propagation in the graphene film (Fig. 1a). The composite layer consists of a block-copolymer derived nanoporous carbon film as well as a multi-walled carbon nanotube mesh. The membranes are mechanically robust and can be successfully pressurized to 5 bar without inducing failure. H_2/CH_4 and H_2/CO_2 selectivities of 11–23 and 5–8, respectively, higher than the corresponding Knudsen selectivities of 2.8 and 4.7, respectively, can be obtained from the centimeter-scale NSLG membranes (Fig. 1b). Finally, we will show the analysis of the concentration of non-selective pores in these membranes using a bimodal pore-size-distribution model. Overall, the approach reported here helps accelerate the adoption of NSLG membranes for gas separation.

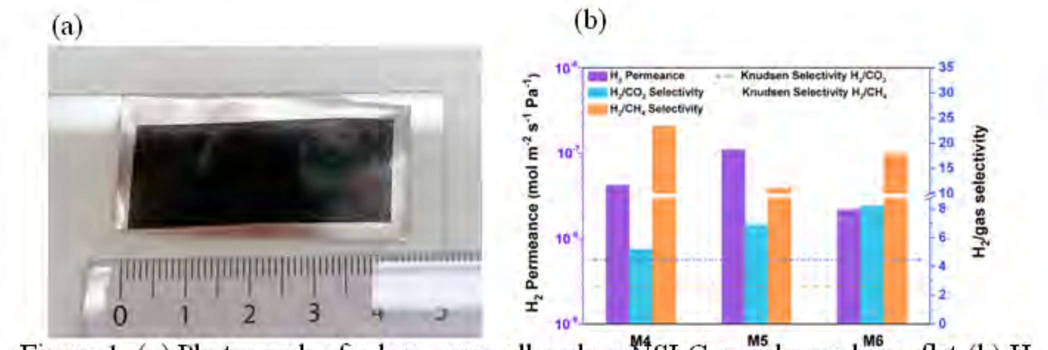

Figure 1. (a) Photograph of a large-area all-carbon NSLG membrane lying flat (b) H_2 permeance and ideal selectivities of H_2 with respect to CH_4 and CO_2 across three graphene membranes using a single-component feed at 100°C. The horizontal dashed lines correspond to the expected Knudsen selectivity between the gas pairs when the effusive transport dominates the overall gas transport.

[1] Lee, W.-C.; Bondaz, L.; Huang, S.; He, G.; Dakhchoune, M. and Agrawal, K.V., Centimeter-Scale Gas-Sieving Nanoporous Single-Layer Graphene Membrane, Submitted

[2] Huang, S.; Dakhchoune, M.; Luo, W.; Oveisi, E.; He, G.; Rezaei, M.; Zhao, J.; Alexander, D. T. L.; Züttel, A.; Strano, M. S.; et al. Single-Layer Graphene Membranes by Crack-Free Transfer for Gas Mixture Separation. *Nat. Commun*. 2018, 9 (1), 2632.

[3] Boutilier, M. S. H.; Hadjiconstantinou, N. G.; Karnik, R. Knudsen Effusion through Polymer-Coated Three-Layer Porous Graphene Membranes. *Nanotechnology* 2017, 28, 184003

Metal soap membranes for gas separation

Q. Liu[1]

[1]EPFL, LAS

Metal soaps, or metal alkanoates, as a kind of liquid crystal when heating, are constructed by metal cations and organic molecules composed of a variety of functional groups linked to hydrocarbon chains.[1-4] They have a bi-layered arrangement with a layer made of metal cations linked with the functional groups and another layer made of lipidic hydrocarbon chains. The metal cations are linked by functional groups, forming a layer of rods/chains and sheets, while the functional groups are co-bonded to hydrocarbon chains, which act as the other layers (Figure 1). Due to the high flexibility of long alkyl chains in the structures, most metal soaps can melt at a certain temperature, forming a disordered/amorphous liquid phase or a mesophase. The liquid phase can be readily quenched by cooling down upon which the disordered structures quickly turn back to the original crystalline state. This presents an opportunity to evaluate this class of material for gas separation membranes especially in the context of large number of possible ordered porous metal soap which could allow separation of a number of gas pairs by size sieving. Additionally, metal soap provide processability advances as one could synthesize membranes by using solid to liquid transition ability of metal soaps, making such membranes easy to scale-up. In this presentation, firstly, I will introduce two facile methods, interfacial crystallization and melting method, to synthesize membranes which constructed by three metal soaps, CaC_{12} ($Ca(SO_4C_{12}H_{25})_2$), ZnC_6 ($Zn(COOC_6H_{13})_2$) and CuC_9 ($Cu(COOC_9H_{19})_2$). Regarding to melting method, the membrane formed by heating the powders of these structures in low temperatures (120 -150 ˚C) in less than 1 hour (Figure 1A). While as to interfacial crystallization, the continuous film is formed on the whole area of water surface in few seconds (which we found to be a facile way to synthesize film with very low thickness). And the film could be easily transported by scooping with any substrate (Figure 1B). Both methods show potential of easy-processability and facile scale-up. Secondly, I will discuss the crystal structures and characterizations of these metal soaps. All of them have pores coming from the gaps around 3 Å, which means they could be used in hydrogen sieving (H_2, 2.89 Å) or carbon capture (CO_2, 3.3 Å). Scanning electronic microscope (SEM) images showed the thickness of these membranes are less than 5 µm (Figure 1C-1E). X-ray diffraction (XRD) data confirmed the high crystallinity of all membranes. Finally, I will discuss the gas separation property of these membranes. Molecular sieving is demonstrated with ideal gas selectivities up to 10.5, 11.3 and 13.0 for H_2/CO_2, H_2/CH_4 and CO_2/N_2, respectively (Figure 1F-1H).

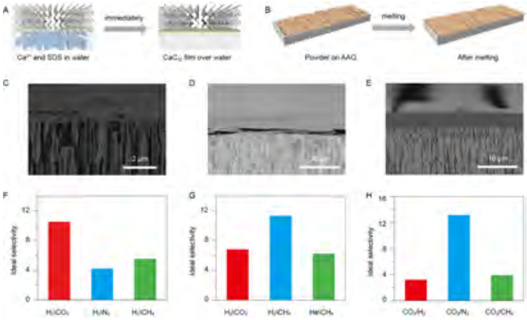

[1] G. Klimusheva, T. Mirnaya, Y. Garbovskiy, *Liq. Cryst. Rev.*, **2015**, 3, 28-57.
[2] R. Corbery, *Curr. Opin. Colloid In. Sci.*, **2008**, 13, 288–302.
[3] V. Luzzati, A. Tardieu, T. Gulik-Krzywicki, E. Rivas, F. Reiss-Husson, *Nature* **1968**, 220, 1351-1352.
[4] J. Peultier, E. Rocca, J. Steinmetz, *Corros. Sci.*, **2003**, 45, 1703–1716.

Direct Co-H exchange of Fluoroarenes mediated by a mixed-metal Na/Co(II) base

A. Logallo[1], E. Hevia[1]*

[1]University of Bern, Department of Chemistry and Biochemistry, Freiestrasse 3, 3012 Bern, Switzerland

Fluorinated organic compounds increasingly gain importance in numerous areas of chemistry and everyday life, as building blocks containing fluorinated entities are of high significance in areas such as materials science, catalysis, medicine, and biochemistry. [1] Deprotonative metallation is a powerful methodology for the functionalization of aromatic molecules, however deprotonation of fluoroarenes using polar organometallic reagens like RLi is particularly challenging due to the lack of stability of the relevant metallated intermediates.

Breaking new ground in this area, this poster presents our findings in the development of a mixed-metal base combining Na and Co(II) in the same molecule that enables the effective and regioselective deprotonation of a range of fluoroarenes while operating at room temperature. Furthermore, NMR spectroscopic and X-ray crystallographic studies have established these reactions constitute the first examples of sodium-mediated-cobaltation (AMM*Co*), where Co assisted by the alkali-metal promotes the direct Co-H exchange process.

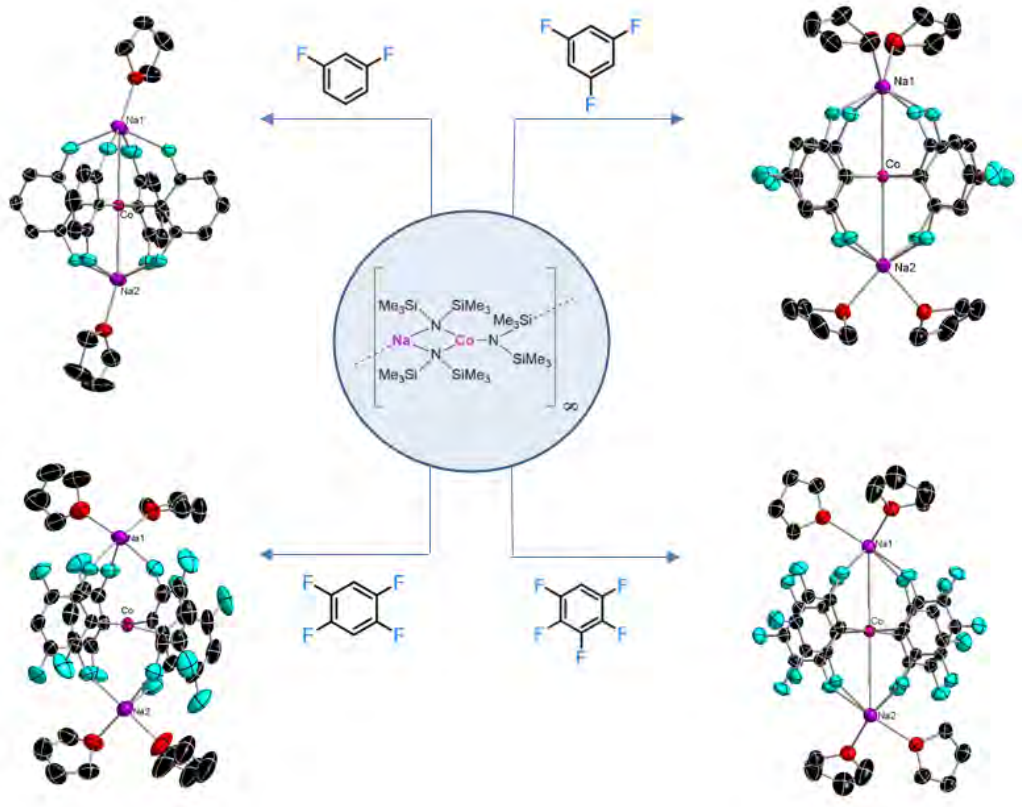

[1] Theresia Ahrens, Johannes Kohlmann, Mike Ahrens, Thomas Braun, *Chemical Reviews,* **2015**, 115, 931

Extremely Large Upper Critical Field in the Isotropic *η*-Carbide Superconductor $Nb_4Rh_2C_{1-\delta}$

K. Ma[1], K. Gornicka[2], R. Lefèvre[1], H. O. Jeschke[3], T. Klimczuk[2], F. O. von Rohr[1,4]*

[1]Department of Chemistry, University of Zurich, CH-8057 Zurich, Switzerland , [2]Faculty of Applied Physics and Mathematics, Gdansk University of Technology, Gdansk 80-233, Poland, [3]Research Institute for Interdisciplinary Science, Okayama University, Okayama 700-8530, Japan, [4] Department of Physics, University of Zurich, CH-8057 Zurich, Switzerland

The upper critical field $H_{c2}(0)$ is a fundamental measure of the strength of superconductivity in a material. It arises due to pair breaking at a limiting field due the Pauli paramagnetism of the electrons. The maximal possible magnetic field strength for this effect is commonly known as the Pauli paramagnetic limit H_{Pauli}, which is given by 1.86Tc. The violation of this limit is rarely observed. Exceptions include some low-temperature heavy-fermionic and some strongly anisotropic superconductors. Here, we show the superconductivity at 9.7 K in the cubic *η*-carbide-type compound $Nb_4Rh_2C_{1-\delta}$. We find that this material has a remarkably high upper critical field of $H_{c2}(0) \approx 33.6$ T, which is exceeding by far the Pauli paramagnetic limit of $\mu_0 H_{\mathrm{Pauli}} \approx 18.1$ T. This material has, at the same time, a lower critical field of only $H_{c1}(0) = 13.6$ mT. This large critical field difference makes it an extreme type-II superconductor with a remarkably short superconducting coherence length and a large superconducting penetration depth λ_{GL}. Determination of the origin and consequences of this effect will represent a significant new direction in the study of critical fields in superconductors. Furthermore, our results show that *η* -carbides are remarkably promising candidates for the preparation of next-generation superconducting magnets.

Mixed Alkali-Zinc Bases in Direct Metallation: Alkyl Versus Amide Kinetic Basicity and Stabilization of Delicate Fluoroarene Anions

P. Mastropierro[1,2], M. Uzealc[2], E. Hevia[1,2]*

[1]Department of Chemistry and Biochemistry, Universität Bern, Freiestrasse 3, 3012, Bern, [2] WestCHEM, Department of Pure and Applied Chemistry, University of Strathclyde, 295 Cathedral Street, Glasgow, G1 1XL, UK

Fluoro-substituted aromatics are being increasingly employed as scaffolds in agrochemicals and active pharmaceutical ingredients. Thus, new regioselective approaches to access functionalized fluorinated aromatic skeletons are in high demand, with special emphasis currently on activating their C-H bonds. Deprotonative metallation of fluoroarenes using conventional s-block bases represents a formidable challenge due to the hypersensitivity of the metallo-intermediates, which have a tendency to undergo decomposition through benzyne formation, concomitant fluoride salt elimination or related cascade processes.[1]

Here we exploit s-block bimetallic cooperative effects in reporting the opening application of a specially designed potassium amido zincate base supported by the sterically demanding bis(amide) ligand $Ph_2Si(NAr^*)_2^-$ (Ar*= 2,6-diisopropyl-phenyl)[2] for regioselective metalation of hypersensitive fluorinated organic building blocks. Overcoming common limitations of standard s-block metallating bases, this system enables reactions to be carried out at room temperature, trapping, and protecting fluoroaryl anions that can then be further functionalized via Negishi cross-coupling protocols.

With more activated substrate like 2’,4’,6’-trimethylacetophenone, this sterically demanding anion demonstrates its non-innocent behaviour in metallation. $Ph_2Si(NAr^*)_2^-$ demonstrates even superior kinetic basicity than the CH_2SiMe_3 alkyl group when part of a heteroleptic zincate.

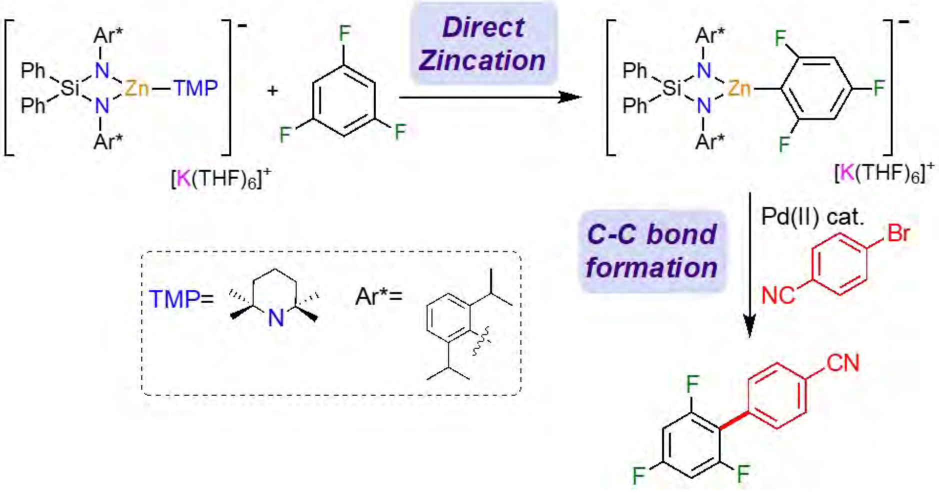

[1] Manfred Schlosser, Laurence Guio, Frédéric Leroux, *J. Am. Chem. Soc.*, **2001**, 123, 3288
[2] Victoria L. Blair, William Clegg, Alan R. Kennedy, Zoe Livingstone, Luca Russo, Eva Hevia, *Angew. Chem. Int. Ed.* **2011**, 50, 9857–9860

N-heterocyclic carbene iron piano stool complexes for lactide polymerisation catalysis

P. V. Nylund[1], M. Albrecht[1]*

[1]Department für Chemie und Biochemie, Universität Bern

Production of cheap durable polymers with many applications such as food packaging, building materials and electronic components mainly depend on petrochemicals and they are difficult to replace. This fossil dependence and the current situation of plastic pollution in most parts of the globe motivates a search of alternative materials.[1-3]. The biodegradable, non-fossil and recyclable polylactic acid already substitutes some fossil derived polymers such as PET.[4,5] Earlier work in our group and others has shown that iron piano stool complexes are active for C=O activation[6–8] and we were curious to see if these type of complexes could also be used for ring-opening polymerisation of lactide.

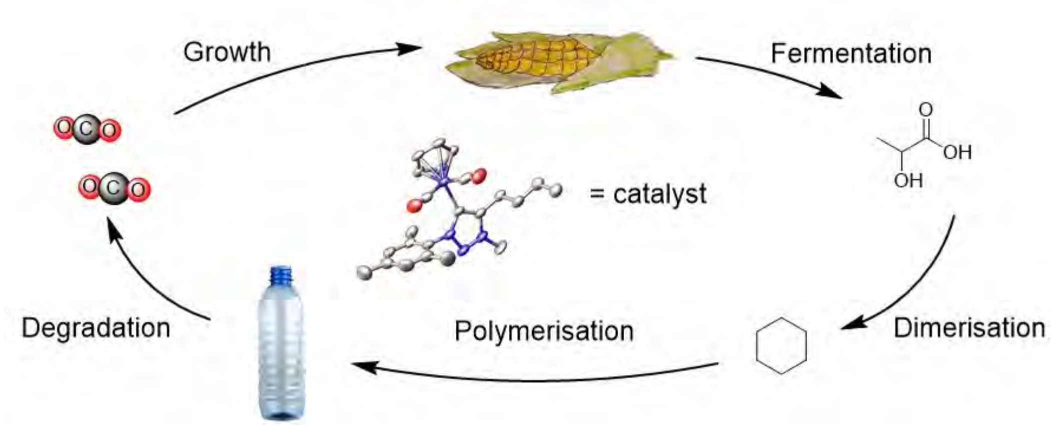

Figure 1 Simplified lifecycle of polylactic acid and an active iron catalyst

Herein we present stable NHC iron(II) piano stool complexes with remarkable LA polymerisation activities. After optimisation, the best complex displayed, to the bes of our knowledge, the highest activity so far.

[1] Steve Allen, Deonie Allen, Vernon R. Phoenix, Gaël Le Roux, Pilar Durántez Jiménez, Anaëlle Simonneau, Stèphane Binet, Didier Galop, *Nat. Geosci.* **2019**, 12, 339–344.
[2] Laurent C.M. Lebreton, Joost van der Zwet, Jan-Willem Damsteeg, Boyan Slat, Anthony Andrady & Julia Reisser, *Nat. Commun.* **2017**, 8, 1–10.
[3] Christian Schmidt, Tobias Krauth,Stephan Wagner, *Environ. Sci. Technol.* **2017**, 51, 12246–12253.
[4] Merjä Itävaara, Sari Karjomaa, Johna-Fredrik Selin, *Chemosphere*, **2002**, 46, 879–885.
[5] Jasim Ahmed, Sunil K. Varshney, *International Journal of Food properties* **2011**, 14, 37-58.
[6] Fan Jiang, David Bézier, Jean-Baptiste Sortais, Christophe Darcel, *Adv. Synth. Catal.* **2011**, 353, 239–244.
[7] Rita Lopes, Mariette M.Pereira, Beatriz Royo, *ChemCatChem* **2017**, 9, 3073–3077.
[8] Chloë Johnson.; Martin Albrecht. *Organometallics* **2017**, 36 , 2902–2913.

Metalla-assemblies for photodynamic therapy

C. Papadimou[1], B. Therrien[1]*

[1]Institute of Chemistry, University of Neuchâtel, Switzerland

Photodynamic therapy (PDT) is a medical treatment for skin disorders, infectious diseases and various types of cancer. PDT acts through a combination of three individually harmless elements: a light-absorbing molecule or photosensitizer (PS), oxygen and a light-source [1]. When the PS is exposed to certain wavelengths of light, it becomes activated from a ground state to an excited one. As the PS turns back to its ground state, it releases energy, which is transferred to oxygen to generate reactive oxygen species, thus mediating cellular toxicity [2]. Water-soluble arene-ruthenium metalla-assemblies can host in their cavity a PS and transport it to the tumor cells, where the PS can be activated and be cytotoxic [3].

A major PDT limitation is hypoxia: a low-oxygen tension condition characteristic of the poor blood-supplied central tumor region [4, 5]. An anthracene molecule can carry $^1O_2$ into cancer cells in the form of an endoperoxide [6]. Consequently, introduction of more $^1O_2$ molecules into solid tumors through the photo-activated Ru-based compounds, followed by application of PDT on the cancer, can possibly treat hypoxic tumors by enhancing the PDT effect.

My project targets the synthesis of anthracene-functionalized-ruthenium metalla-assemblies for PDT applications. These new metalla-assemblies can in principle augment the number of $^1O_2$ molecules in tumor cells, and release these killing agents near the photosensitizer hosted in the metalla-cage, thus bringing together the PS and $^1O_2$.

[1] A.C.E. Moor, B. Ortel, T. Hasan, *Photodynamic Therapy*, Royal Society of Chemistry, Cambridge, **2003**, pp. 19–58.
[2] D.E.J.G.J. Dolmans, D. Fukumura, R.K. Jain, *Nature Reviews Cancer,* **2003**, 3, 380-387.
[3] F. Schmitt, J. Freudenreich, N.P.E. Barry, L. Juillerat-Jeanneret, G. Süss-Fink, B. Therrien, *J. Am. Chem. Soc.,* **2012**, 134, 754–757.
[4] D. Ganten, K. Ruckpaul, Eds., *Encyclopedic Reference of Genomics and Proteomics in Molecular Medicine*, Springer-Verlag, Berlin, Heidelberg, **2006**, pp 853–853.
[5] A. Sharma, J.F. Arambula, S. Koo, R. Kumar, H. Singh, J.L. Sessler, J.S. Kim,*Chem. Soc. Rev.*, **2019**, 48, 771-813.
[6] M. Gaschard, F. Nehzat, T. Cheminel, B. Therrien, *Inorganics*, **2018**, 6, 97.

Spin-flip luminescence in six-coordinate complexes of nickel(II): attempts and challenges

C. Reber[1], C. Dab[1], C. Förster[2], K. Heinze[2]

[1]Université de Montréal, Département de chimie, [2]Johannes Gutenberg-Universität Mainz, Departement für Chemie

Luminescent complexes of earth-abundant first-row transition metals are of renewed interest due to their spectroscopic and photochemical properties.[1-4] Particularly, chromium(III) complexes with *N*,*N'*-dimethyl-*N*,*N'*-dipyridine-2-yl-pyridine-2,6-diamine (ddpd) and related ligands have been widely studied and show intense spin-flip luminescence. $Ni(ddpd)_2^{2+}$ has a strong ligand field and spin-flip luminescence can be expected, as shown in the left-hand scheme.

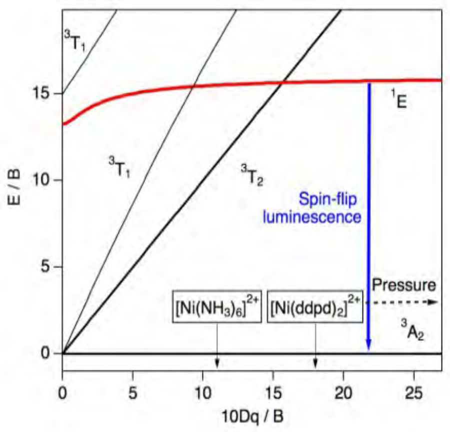

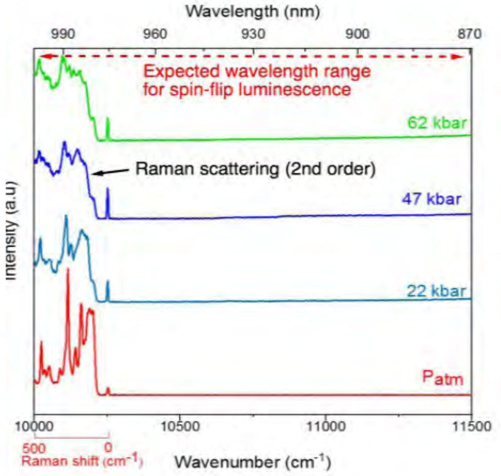

We have attempted to observe spin-flip luminescence for the $Ni(ddpd)_2^{2+}$ complex [5] but have not detected any signal in the wavelength range expected, even at high external pressure (right-hand figure).[6] As pressure increases, Raman spectra broaden, documenting a deterioration of the crystal quality. This also leads to defect sites that often quench luminescence at pressures well below 100 kbar. The presentation highlights the crucially different excited-state landscapes leading to the luminescence properties indicating how to potentially achieve spin-flip luminescence in nickel(II) complexes.

[1] Sven Otto, Markus Grabolle, Christoph Förster, Christoph Kreitner, Ute Resch-Genger, Katja Heinze, *Angewandte Chemie International Edition*, **2015**, 54, 11572–11576.
[2] Kasper Skov Kjær, Nidhi Kaul, Om Prakash, Pavel Chábera, Nils W. Rosemann, Alireza Honarfar, Olga Gordivska, Lisa A. Fredin, Karl-Erik Bergquist, Lennart Häggström, Tore Ericsson, Linnea Lindh, Arkady Yartsev, Stenbjörn Styring, Ping Huang, Jens Uhlig, Jesper Bendix, Daniel Strand, Villy Sundström, Petter Persson, Reiner Lomoth, Kenneth Wärnmark, *Science*, **2019**, 363, 249-253.
[3] Christoph Förster, Katja Heinze, *Chemical Society Reviews*, **2020**, 49, 1057-1070.
[4] Sven Otto, Joe P. Harris, Katja Heinze, Christian Reber, *Angewandte Chemie International Edition*, **2018**, 57, 11069-11073.
[5] Matthias Dorn, Katharina Mack, Luca M. Carrella, Eva Rentschler, Christoph Förster, Katja Heinze, *Zeitschrift für anorganische und allgemeine Chemie*, **2018**, 644, 706–712.
[6] Chahinez Dab, Katja Heinze, Christian Reber et al., in preparation.

Bioinspired Metal-Complexes as Chelators of Bacterial Metallo-β-Lactamase Zinc Ions

J. V. Schwarte[1], B. Giese[1]*

[1]Fromm Group, Department of Chemistry, University of Fribourg

The bacterial metallo-β-lactamases are a current and pressing target for drug design. Indeed, they induce antibiotic resistance by participating in the hydrolysis of a whole class of antibiotics, the β-lactams (except monobactams), which are currently used worldwide.[1]

As illustrated below, their mechanism of action implies the participation of water molecules and zinc ions.

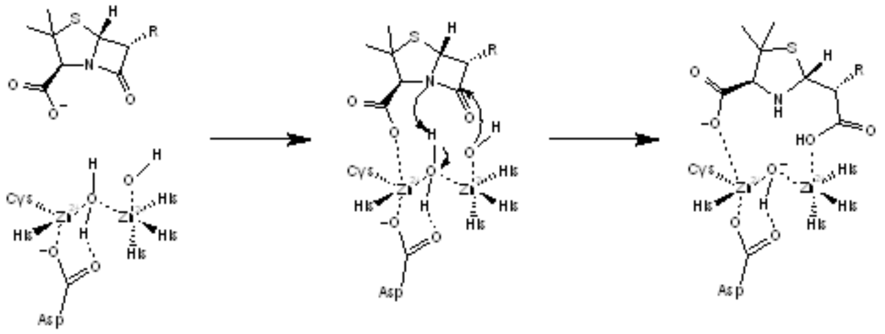

Figure 1: Hydrolysis mechanism of β-lactam antibiotics inside the active site of metallo-β-lactamase, (inspired from M-R. Meini, L. I. Llarrull, A. J. Vila, *FEBS Letters* **2015,** 589, 3419–3432).

One possible way to inactivate these metallo-proteins could be the use of chelating drugs to remove the ions.[2] Therefore, after synthesizing a model peptide of the active site, the project aims at the extraction of the zinc ions, and their replacement by a ligand or other metal ions. This requires to determine the affinity of the model peptide and the potential ligands for the tested metal ions.

[1] Yusof, D. T. C. Tan, O. K. Arjomandi, G. Schenk, R. P. McGeary, *Bioorganic and Medicinal Chemistry Letters,* **2016**, 26, 1589-1593.
[2] N. Mitic, M. Miraula, C. Selleck, K. S. Hadler, E. Uribe, M. M. Pedroso, G. Schenk, *Advances in Protein Chemistry and Structural Biology,* **2014**, 97, 49-81.

Synthesis of crystalline atom-thick poly(triazine imide) nanosheets for energy-efficient molecular separation

L. F. Villalobos[1], K. V. Agrawal[1]*

[1]Laboratory of Advanced Separations (LAS), EPFL Lausanne

Poly(triazine imide) or PTI (Figure 1A,B),[1] one of the few truly crystalline graphitic carbon nitrides synthesized so far, is a highly promising material for energy storage and conversion, sensors, and energy-efficient two-dimensional membranes.[2] PTI is an extremely stable material that can withstand acidic and basic environments,[3] as well as temperatures of up to 600 °C. [4] This opens up the possibility of using PTI films for H^+ and OH^- transport in electrolytic cells, and to recover H_2 directly from the effluent of the steam reforming process without having to cool it down. However, the full potential of PTI can only be harnessed by (i) developing a scalable solid-state chemistry for the layered PTI, (ii) exfoliating PTI crystals into single-layer nanosheets and, (iii) developing self-assembly strategies to process such nanosheets into coatings or thin films with a controlled number of layers. In this presentation, I will discuss our recent success in i) synthesizing crystalline PTI in ambient-pressure conditions, ii) efficient exfoliation of PTI to single-layer, and iii) fabrication of exfoliated PTI-based membranes for hydrogen sieving [5]. Currently, layered-PTI is synthesized in potentially unsafe vacuum ampules in milligram quantities. Its crystallization takes place in molten LiCl where the role of molten salt is widely believed to be that of a solvent. Here, I will discuss our results that negates this hypothesis and show that the role of molten LiCl is akin to a structure directing agent where Li^+ and Cl^- facilitate an ordered condensation of melam. I will discuss our scalable reactor design which operates at ambient pressure, and yields several grams of layered PTI platelets in a single batch with 70% yield (Figure 1C). I will further discuss high-yield exfoliation of PTI using an anhydrous solvent strategy. The triangular nanopores of PTI have never been observed before, attributing to the fact that single-layer PTI have not been isolated so far. A one-step exfoliation using anhydrous DMAc will be discussed which leads to a high percentage of atom-thick PTI nanosheets (Figure 1D) evidenced by the observation of the triangular nanopores of graphitic carbon nitride for the first time (Figure 1E and F). The strong interaction of DMAc molecules with Li+ ions drives the exfoliation at high temperatures. Finally, gas permeation studies and first-principles simulations demonstrating the ability of PTI nanopores to sieve He and H_2 from larger molecules will be discussed (Figure 1G and H).

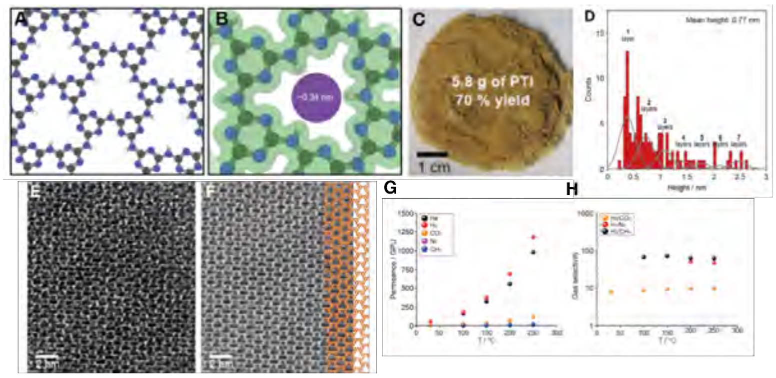

Fig. 1. Structure of single-layer PTI lattice (A) and electron-density gap in PTI (B). C) Picture showing the high yield of layered-PTI. D) Thickness histogram of exfoliated PTI nanosheets (n>100). A sum of Gaussians with a FWHM of 0.35 nm shows the approximate range of bins that correspond to each number of layers. E) HRTEM image of a single-layer PTI nanosheet, and (F) its corresponding filtered image with the structure of single-layer PTI superimposed (C and N atoms colored in red and yellow, respectively). Permeance of He, H_2, CO_2, N_2 and CH_4 as a function of temperature (G), and corresponding H_2/CH_4, H_2/N_2 and H_2/CO_2 ideal selectivities (H).

[1] E. Wirnhier, et al., *Chem. - A Eur. J.* **2011**, *17*, 3213.; [2] F. K. Kessler, et al., *Nat. Rev. Mater.* **2017**, *2*, 17030; [3] K. Schwinghammer, et al., *Angew. Chemie Int. Ed.* **2013**, *52*, 2435; [4] T. S. Miller, et al., *Nano Lett.* **2017**, *17*, 5891; [5] L.F. Villalobos, et al., *Sci. Adv.* **2020**, *6*, eaay9851.

Stabilizing Molecular Complexes of Terbium(IV) and Accessing Molecular Complexes of Praseodymium in the +IV Oxidation State.

A. R. Willauer[1], C. T. Palumbo[1], R. Scopelliti[1], F. Fadaei-Tirani[1], I. Zivkovic[2], I. Douair[3], L. Maron[3], M. Mazzanti[1]*

[1]Institut des Sciences et Ingénierie Chimiques, EPFL, [2]Institute of Physics, EPFL, [3]Institut National des Sciences Appliquées, Toulouse

The molecular chemistry of lanthanide ions is dominated by the +III oxidation state. In contrast, molecular complexes of lanthanides in the +IV oxidation state were limited to cerium for a long time. It is only in 2019 that the first two examples of molecular complexes of Tb(IV), [Tb(OSi(O^{t}Bu)$_3$)$_4$], **2-Tb$^{\mathbf{OtBu}}$**,[1] and [Tb(NP(1,2-bis-^{t}Bu-diamidoethane)(NEt$_2$))$_4$], **2-Tb$^{\mathbf{N=P}}$**,[2] were isolated. However, attempts to access the analogue "[Pr^{IV}(OSi(O^{t}Bu)$_3$)$_4$]" failed and only resulted in the isolation of a trivalent species. Here we show that Tb(IV) chemistry can be extended to the monodentate triphenylsiloxide ligand with the isolation of the third example of a Tb(IV) molecular complex [Tb(OSiPh$_3$)$_4$(MeCN)$_2$], **2-Tb$^{\mathbf{Ph}}$**, showing an unsaturated Tb coordination sphere and an overall higher thermodynamic and kinetic stability compared to **2-Tb$^{\mathbf{OtBu}}$**.[3] More importantly, we discovered that this ligand can also lead to the isolation of the first molecular complex of praseodymium in the +IV oxidation state [Pr(OSiPh$_3$)$_4$(MeCN)$_2$], **2-Pr$^{\mathbf{Ph}}$**.[4]

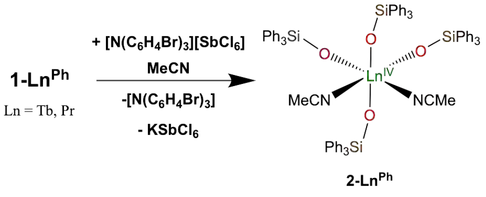

2-Ln^{Ph}

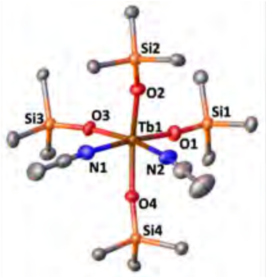

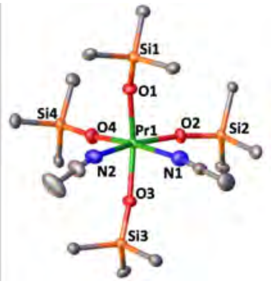

Oxidation of [KLn(OSiPh$_3$)$_4$(THF)$_x$] (Ln = Tb, x = 1; Ln = Pr, x = 3), **1-Ln$^{\mathbf{Ph}}$** with [N(C$_6$H$_4$Br)$_3$][SbCl$_6$] in MeCN allowed the isolation of **2-Tb$^{\mathbf{Ph}}$** and **2-Pr$^{\mathbf{Ph}}$** in 24 % and 55 % yield respectively. Both **2-Tb$^{\mathbf{Ph}}$** and **2-Pr$^{\mathbf{Ph}}$** complexes were characterized by X-ray crystallography, cyclic voltammetry, magnetometry, electron paramagnetic resonance and density functional theory calculations corroborating the +IV oxidation state. Solution stability studies in THF showed a significantly lower decomposition rate for complex **2-Tb$^{\mathbf{Ph}}$** compared to **2-Tb$^{\mathbf{OtBu}}$** suggesting a more important stabilization of the +IV oxidation state by the supporting triphenylsiloxide ligands. Furthermore, cyclic voltammetry experiments on **2-Tb$^{\mathbf{Ph}}$** shows redox potential values ~ 0.4 V smaller compared to **2-Tb$^{\mathbf{OtBu}}$**. More importantly, a stabilization of the + IV oxidation state was noticed in the presence of outersphere countercations compared to alkali metal ions. Indeed, cyclic voltammograms of **1-Tb$^{\mathbf{Ph}}$**, presenting a bound K, or **2-Tb$^{\mathbf{Ph}}$** measured in the presence of Na$^+$ electrolyte show a reduction potential shifted ~ 0.7 V towards more positive values compared to **2-Tb$^{\mathbf{Ph}}$** measured in a NBu$_4$$^+$ electrolyte. DFT calculations assigned the increased stability of **2-Tb$^{\mathbf{Ph}}$** to a strong π(O–Tb) interaction. Complex **2-Pr$^{\mathbf{Ph}}$** shows an oxidation potential wave at a value 0.27 V more positive than **2-Tb$^{\mathbf{Ph}}$** which is consistent with the slight difference in the calculated redox potentials of the Ln(IV)/Ln(III) couples (Ln = Tb, Pr). Furthermore, computational studies shows that the unpaired spin density is only located at the metal centers and that **2-Pr$^{\mathbf{Ph}}$** displays an increased covalent interaction with the ligand compared to **2-Tb$^{\mathbf{Ph}}$**. These new results provide key information in lanthanides tetravalent chemistry and provide a new area of study for redox reactivity and separation chemistry.

[1] Palumbo C. T. *et al.*, *J. Am. Chem. Soc.*, **2019**, 141, 9827-9831. [2] Rice N. T. *et al.*, *J. Am. Chem. Soc.*, **2019**, 141, 13222-13233.
[3] Willauer A. R. *et al.*, *Angew. Chem. Int.Ed.*, **2020**, 59, 3549-3553. [4] Willauer A. R. *et al.*, *J. Am.*

Chem. Soc., **2020**, 142, 5538-5542.